POLITECNICO
MILANO 1863

SCUOLA DI INGEGNERIA INDUSTRIALE
E DELL'INFORMAZIONE

Displacement detection of an oscillator based on a nano-mechanical qubit

Tesi di Laurea Magistrale in
Engineering Physics - Ingegneria Fisica

Andrea Amico, 952805

Abstract: In recent years mechanical oscillators have been proposed as an alternative for the implementation of quantum computing. One of the proposals for a nanomechanical qubit is a suspended carbon nanotube, in which a double quantum dot is integrated using gate voltages. In this work we study one of the possible read-out methods of this mechanical oscillator, based on a single electron transistor (SET). The SET, composed of a metallic island isolated by tunnelling junctions, allows the passage of one electron at a time, thus in principle being suitable for high sensitivity in the detection of the oscillator displacement. Here, we compute the back action of the SET on the oscillator, presenting the oscillator excitation in terms of an effective temperature. We show the exponential dependence of the effective temperature on the voltage bias applied at the SET electrodes. The dependence of the back action on the energy level of the SET metallic island is also retrieved. Finally we compute the expression of the current of the SET, retrieving the dependence on the oscillator displacement. This computation is done both semiclassically and with a full quantum description of the oscillator-SET coupling. We describe the sensitivity of the SET trough the derivative of the SET conductance with respect to the oscillator displacement, and we express this figure of merit as a function of the energy level in the metallic island and the tunneling rates This allows us to estimate the behaviour of the device in different operational regimes, defined by parameters such as the applied voltage on the SET and by the physical values characteristic of the oscillator-SET system.

Advisor:
Prof. Andrea Crespi

Co-advisors:
Prof. Fabio Pistolesi

Academic year:
2022-2023

Key-words: nanomechanical oscillator, carbon nanotube, single electron transistor, qubit, quantum noise

1. Introduction

Quantum computing has raised interest due to its potential to solve problems that are intractable for classical computers. Unlike classical computers that use binary digits (bits) to represent information, quantum computers use two level quantum systems (qubits) that can be in a superposition of both 0 and 1 simultaneously, thanks to the properties of quantum mechanics. This enables to perform multiple calculations in parallel, leading to exponential speedup in certain computations and tasks. On the other hand this new technology has to face significant challenges to realize its physical implementation. In particular quantum systems easily lose their characteristic superposition when interacting with the environment: this mechanism is called decoherence and is one of the main obstacles to quantum computing implementation. A qubit has to be read-out and manipulated, in other words it has to be subject to interactions without the superposition being destroyed.
There are several types of qubits that have been proposed and demonstrated experimentally, such as superconducting micro circuits, trapped ions, and quantum dots. The already mentioned challenges make it difficult for all these qubits to be assembled in circuits, because scaling up the system size makes it more sensitive to decoherence. In this frame, nanomechanical qubits have been proposed as a promising platform for quantum information processing and storage, due to their unique features. Since any force lead to a mechanical motion, they can in principle couple to different force fields. Furthermore, they exhibit large quality factors and long coherence times. In addition they are compatible with modern microfabrication of resonators [1]. The resonator that we explore here is a suspended carbon nanotube whose oscillation modes can be used to encode information. Anharmonicity is introduced to make the energy levels unevenly spaced and to make it possible to isolate a two level system to be used as a qubit. In detail, anharmonicity is induced by the presence of a double quantum dot, created by applying voltages trough gates all along the nanotube. As always, the main challenge is the read out and manipulation of this qubit since the oscillating frequency can extend up to the order of the GHz. Using a resonant microwave cavity was proposed as a solution for qubit readout.
In this thesis work we will investigate an alternative solution based on a single electron transistor (SET). A SET consist of a metallic island of micrometric size isolated from the rest of the circuit by two tunneling junctions. The main feature which makes this device interesting is the ability of controlling the current flow up to single electron accuracy. This is possible when the central island is small enough that well separated discrete energy levels appear. In detail, in this work we are going to explore the coupling between the SET and the nanomechanical qubit (NMQbit) via theoretical modeling, with the aim of study the backaction of the SET on the NMQbit, and the sensitivity of SET current to the oscillator displacement. This will asses the feasibility of this device, and suggest suitable operating regimes.
The research work discussed in this thesis was conducted during my stay at the Laboratoire Onde et Matière d'Aquitaine (LOMA), from March to August 2022, under the supervision of Prof. Fabio Pistolesi whom I sincerely thank.

2. Basic formalism of Quantum Mechanics

The new ideas and concept carried within quantum mechanics require a different mathematical formalism with respect to classical mechanics. In this section the aim is not a complete overview on the subject, rather it is to highlight in the most straight forward way the key features of Quantum Mechanics that are going to be exploited in this work.

2.1. Quantum States and Observables

In Quantum Physics, states of a system are completely represented by unitary-norm vectors in the Hilbert space associated to the system. They are indicated with kets $|\psi\rangle$. The time evolution of these states in quantum mechanics is given by the solution of the Schrodinger equation:

$$\hat{H}|\psi(t)\rangle = i\hbar\frac{\partial|\psi(t)\rangle}{\partial t}. \tag{1}$$

Here, $\hat{H}$ is the so called Hamiltonian operator, i.e. the operator corresponding to the total energy of the system, and $\hbar = \frac{h}{2\pi}$ with h Planck's constant. We can introduce the time evolution operator, which is a unitary operator that describes the time evolution of a system.

$$|\psi(t)\rangle = \hat{U}|\psi(0)\rangle. \tag{2}$$

For a time independent Hamiltonian the solution of the Schrodinger equation reads:

$$|\psi(t)\rangle = e^{-i\frac{\hat{H}}{\hbar}t}|\psi(0)\rangle. \tag{3}$$

Therefore:

$$\hat{U} = e^{-i\frac{\hat{H}}{\hbar}t}. \tag{4}$$

As a further note we recall that unitary transformation operators in a linear space have the property:

$$\hat{U}^{\dagger}\hat{U} = \hat{I} \tag{5}$$

In quantum mechanics, any physical observable is associated with a Hermitian operator in the Hilbert space of the system. For each operator it is possible to define a set of eigenstates. The collection of eigenvalues associated to the eigenstates represent all the possible outcomes from a measurement of the observable. It is therefore possible to write an eigenvalue equation for an operator:

$$\hat{A}|\phi_n\rangle = a_n|\phi_n\rangle, \tag{6}$$

here $|\phi_n\rangle$ is an orthonormal basis of eigenvectors of the operator A. If the operator is Hermitian, as it always is when it represents an observable, the eigenvalues will be real and the eigenvectors will form a complete orthonormal set in the Hilbert space associated to the system.

Coherent Superposition

Being the Hilbert space linear it is possible to express any wavevector corresponding to a physical state as a linear superposition of wavevectors of any basis.

$$|\psi\rangle = \sum_n c_n(t)|\phi_n\rangle. \tag{7}$$

Here c_n are complex coefficients. These are the formal terms of the *superposition principle* yielding to the conclusion that the superposition state $|\psi\rangle$ correspond to a physical state of the system in the same way as $|\phi_n\rangle$ do. In other words, to highlight the most counter intuitive aspect, each of the states composing the superposition is simultaneously present. Note that, if the state composing the superposition are solutions of the Schrodinger equation, so will be the resulting state. Before going on, we say that for each *ket* in the Hilbert space there is an hermitian conjugate (i.e. the complex-valued vector is transposed and conjugated) that is called *bra*, $\langle\psi|$. The product between a bra and a ket is called inner product. This being said, the expression for the coefficients of Eq. (7) takes this form:

$$c_n(t) = \langle\phi_n|\psi\rangle = \sum_k c_k(t)\langle\phi_n|\phi_k\rangle, \tag{8}$$

they can be thought as the projection of ψ over the $n-th$ vector composing the basis. Their square modulus $|c_n(t)|^2$ is the probability to find the system in the n-th eigenstates at a given time when measured. These can be referred to as Born probabilities. To confirm that we define the projection operator:

$$P_n = |\phi_n\rangle\langle\phi_n|, \tag{9}$$

it is easy to see that we get:

$$|c_n(t)|^2 = \langle\psi|P_n|\psi\rangle. \tag{10}$$

Let's introduce the quantum average $\langle A\rangle$ also known as expectation value: the average over all possible outcomes a_n of a measurement weighted by the corresponding probabilities:

$$\langle A\rangle = \sum_n a_n|c_n(t)|^2 = \sum_n a_n\langle\psi|P_n|\psi\rangle = \langle\psi|\sum_n a_n P_n|\psi\rangle. \tag{11}$$

Having said that $\{\phi_n\}$ constitute a complete basis yield to defining the identity operator as follows:

$$\hat{I} = \sum_n |\phi_n\rangle\langle\phi_n| = \sum_n P_n, \tag{12}$$

eventually obtaining the expression for the expectation value:

$$\langle A\rangle = \langle\psi|A|\psi\rangle. \tag{13}$$

Note that $A = \sum_n a_n|\phi\rangle\langle\phi|$ is the spectral decomposition of the operator $\hat{A}$. Note also that being the basis complete yield to $\sum_n |c_n(t)|^2 = 1$, which means that the probabilities are normalized: the probability of obtaining an outcome from a measurement of the observable is equal to 1. This is consistent with:

$$\langle\psi|\psi\rangle = \sum_n |c_n(t)|^2 = 1. \tag{14}$$

Let's now consider a system in a two state superposition:

$$|\Psi(t)\rangle = \lambda_1(t)|\psi_1\rangle + \lambda_2(t)|\psi_2\rangle, \tag{15}$$

and let's consider the probability of obtaining a certain measurement outcome:

$$|\langle\phi_n|\Psi(t)\rangle|^2 = |\lambda_1|^2|\langle\phi_n|\psi\rangle|^2 + |\lambda_2|^2|\langle\phi_n|\psi_2\rangle|^2 + 2Re\left\{\lambda_1(t)^*\lambda_2(t)\langle\psi_1|\phi_n\rangle\langle\phi_n|\psi_2\rangle\right\} \tag{16}$$

The last term is called an interference term. It is a purely quantum mechanical trait. The probability of obtaining a certain measurement does not only depend on the the square moduli of the coefficients λ_1 and λ_2, but also on the relative phase between these complex numbers. Whenever we find a superposition that shows a coherent relation between the phase terms of the states, we have a coherent superposition. The persistence of this coherence when a state interacts with another one is a key aspect that this work partially tries to investigate. We have said that the Hamiltonian operator represents the total energy of a system. Let's consider now a system interacting with another one. The total Hamiltonian will be given by the unperturbed Hamiltonian of the two systems:

$$\hat{H}_0 = \hat{H}_{s1} + \hat{H}_{s2}, \tag{17}$$

plus the so called interaction Hamiltonian $\hat{H}_I$ that will depend on the type of interaction, having:

$$\hat{H} = \hat{H}_0 + \hat{H}_I \tag{18}$$

Time dependence

Let's now clarify how time dependence is addressed in quantum mechanics: there are three equivalent ways or *pictures*.
The first we are going to see is the Schrodinger picture in which time dependence is held in the wavefunction, solution of the Schrodinger equation, while operators remain constant.

$$|\psi(t)\rangle = e^{-i\frac{\hat{H}}{\hbar}t}|\psi(0)\rangle \tag{19}$$

The expectation value is defined as:

$$\langle\hat{O}\rangle = \langle\psi(t)|\hat{O}|\psi(t)\rangle = \langle\psi|e^{i\frac{\hat{H}}{\hbar}t}\hat{O}e^{-i\frac{\hat{H}}{\hbar}t}|\psi\rangle \tag{20}$$

Then we introduce the Heisenberg picture, in which the wavefunction is constant and the operators are evolving in time:

$$\hat{O}(t) = e^{i\frac{\hat{H}}{\hbar}t}\hat{O}e^{-i\frac{\hat{H}}{\hbar}t}. \tag{21}$$

Here the expectation value is computed trough:

$$\langle\hat{O}(t)\rangle = \langle\psi|\hat{O}(t)|\psi\rangle = \langle\psi|e^{i\frac{\hat{H}}{\hbar}t}\hat{O}e^{-i\frac{\hat{H}}{\hbar}t}|\psi\rangle \tag{22}$$

Lastly we have the so called Interaction picture, that can be seen as an intermediate representation between the previous two. As the name suggests, is useful in dealing with dynamics due to interactions. Therefore the Hamiltonian will be written as: $H = H_0 + H_I$. In this frame H_0 usually is the unperturbed part, and H_I the interaction Hamiltonian. Being $|\psi(t)\rangle_S$ the time dependent state vector in the Schrodinger picture, the state vector in the interaction picture is defined from it with an additional timer dependent unitary transformation:

$$|\psi_I(t)\rangle = e^{-i\frac{\hat{H}_0}{\hbar}t}|\psi_S(t)\rangle. \tag{23}$$

Time dependence of operators is given by:

$$\hat{O}(t) = e^{i\frac{\hat{H}_0}{\hbar}t}\hat{O}e^{-i\frac{\hat{H}_0}{\hbar}t}. \tag{24}$$

Here the operator is not dependent in time because usually this is the case. An exception would be that of the density matrix operator, which will be later introduced.

2.2. Entanglement

Entanglement is a key aspect to understand when dealing with composite quantum systems. It is, in Erwin Schrödinger words, *not one but rather the characteristic trait of quantum mechanics*. Let's consider a bipartite system, i.e. two subsystems S and E composing a system W. Then the associated Hilbert space will be given by the following tensor product:

$$\hat{H}_w = \hat{H}_s \otimes \hat{H}_e, \tag{25}$$

whose basis set can be constructed from tensors products of the basis vectors of $\hat{H}_s$ and $\hat{H}_e$, here assumed both n-dimensional.

$$\{|e_n\rangle\}, \{|s_n\rangle\}. \tag{26}$$

A generic state vector $|w\rangle$ is written as of W is written as $|w\rangle = \sum_{i,j} |e_i\rangle \otimes |s_j\rangle$ and is said to be *entangled* with respect to S and E if it cannot be written as a tensor product of different and separable state vectors of the two subsystems.
If we could write $|w\rangle = |e\rangle \otimes |s\rangle$, then the state would be separable. When the state is entangled, it is impossible to look at the subsystems as separate entities. They can only be described by a global composite quantum state. The most adopted example is that of two spin-$\frac{1}{2}$ particles. We will refer to them via the orthogonal basis $|0\rangle$ and $|1\rangle$, corresponding to spin up and down along some given axis, in a two dimensional Hilbert space. The four entangled states arising from this configurations are called Bell states and are the following:

$$|\phi^{\pm}\rangle = \frac{1}{\sqrt{2}}(|0\rangle_1|0\rangle_2 \pm |1\rangle_1|1\rangle_2), \tag{27}$$

$$|\psi^{\pm}\rangle = \frac{1}{\sqrt{2}}(|0\rangle_1|1\rangle_2 \pm |1\rangle_1|0\rangle_2), \tag{28}$$

with 1,2 referring to the two particles. In practice one of these states can be obtained if two particles in a superposition of states $|\Psi^{\pm}\rangle = \frac{1}{\sqrt{2}}(|0\rangle \pm |1\rangle)$ are made to interact, without neither of the two collapsing in one of the two states. The measurement of one state will therefore allow the observer to automatically know the other.
Bell states are defined as maximally-entangled. It is to say, by observing one of the two subsystem the observer will learn everything about the other one. This relies both on the fact that the states of the two particles are one-to-one correlated and that the basis on which states are defined is orthogonal.
Consider the entangled state $|w\rangle$ composed by two sub states:

$$|w\rangle = \frac{1}{\sqrt{2}}(|e_1\rangle|s_1\rangle \pm |e_2\rangle|s_2\rangle), \tag{29}$$

where the states $|e_i\rangle$, with $i = 1, 2$, are not mutually orthogonal, the larger is their overlap the more difficult is to distinguish the two states in a projective measurement.As a consequence it will be also impossible to distinguish with certainty between the states of the system $|s_1\rangle$ and $|s_2\rangle$. In this case the *environment* E encodes little distinguishing information about S. The amount of information learned by the environment about the system increases with the entanglement. Entanglement lead to the system losing its individuality, and won't be possible to describe it as a coherent superposition of states belonging to just the basis set of $\hat{H}_s$. For an entangled state coherence is said to be shared with the environment, eventually leading to decoherence.

2.3. Density matrix description

So far we have considered systems in pure states, i.e. the quantum state vector $|\psi\rangle$ encapsulate the maximum knowledge about the state of the physical system. If instead there is a lack of information about the system, i.e. the system is in one of the $|\psi_i\rangle$ pure states, but it is not known in which, the quantum state can be described by a weighted mixture of these states. This is called a mixed state and it is not possible to describe it in terms of a wavevector. In order to describe it we introduce the density operator defined as:

$$\rho = \sum_k p_k |\psi_k\rangle\langle\psi_k|, \tag{30}$$

where p_i is the probability of sampling from the population of different quantum state the state $|\psi_k\rangle$. Note that the configuration just described represent a classical ensemble, with the probabilities $p_i \geq 0$ being of completely different nature from the probability $|c_n|^2$ that is related to the process of quantum mechanical measurement

of a superposition of states.
In this frame the expectation value of an observable O will be:

$$\hat{O} = \sum_k p_k \langle \psi_k | \hat{O} | \psi_k \rangle. \tag{31}$$

If we now define a complete basis set of eigenvectors of $\hat{O}$, $\{|\phi_n\rangle\}$, it is possible to write:

$$\langle \hat{O} \rangle = \sum_{k,n} p_k \langle \phi_n | \psi_k \rangle \langle \psi_k | \hat{O} | \phi_n \rangle = \sum_n \langle \phi_n | \hat{\rho} \hat{O} | \phi_n \rangle. \tag{32}$$

Therefore:

$$\langle \hat{O} \rangle = Tr(\rho \hat{O}). \tag{33}$$

where $Tr(\rho\hat{O})$ is the trace operation of the product $\rho\hat{O}$. Since the average value of an observable can be always obtained with this operation, we can say that ρ must contain all the physically relevant information that we can learn about a system.
We can also define the density matrix for pure states as:

$$\rho = |\psi\rangle\langle\psi|. \tag{34}$$

In this specific case, writing the state as a superposition $|\psi\rangle = \sum_i c_i |\psi\rangle$ we get:

$$\rho = \sum_{i,j} c_i c_j^* |\psi_i\rangle\langle\psi_j|. \tag{35}$$

Properties

The density matrix has characteristics worth mentioning is Hermitian: let's consider its elements, obtained via matrix representation over the orthonormal basis$\{|\phi_n\rangle\}$:

$$\rho_{i,j} = \sum_k p_k c_{ki} c_{kj}^*. \tag{36}$$

From the above expression it can be demonstrated that ρ is indeed hermitian.
Moreover $Tr(\rho) = 1$, which can be proven exploiting the Eq. (36) :

$$Tr(\rho) = \sum_i \rho_{i,i} = \sum_k p_k \sum_i |c_{ki}|^2 = 1. \tag{37}$$

If we now consider a pure state, it can be proven that $\rho^2 = \rho$, therefore $Tr(\rho^2) = Tr(\rho) = 1$. For a mixed state instead it is found that $Tr(\rho^2) \leq 1$. This constitute an important yet simple criterion to determine the degree of mixedness of a state. The more a state is mixed, the less information is retained about its preparation, the smaller will be the value of $Tr(\rho)$.
Density matrix elements have specific physical meaning.
Diagonal elements are referred to as populations, and represent the probability to measure the system in the state $|phi_i\rangle$. They are written as:

$$\rho_{i,i} = \sum_k p_k |c_{ki}|^2. \tag{38}$$

The off diagonal terms are referred to as coherence elements or *coherences*. They represent the phase relation between two states $|\phi_i\rangle$ and $|\phi_j\rangle$. They read:

$$\rho_{i,j} = \sum_k p_k c_{ki} c_{kj}^*. \tag{39}$$

These elements are present for any state of the statistical mixture containing a linear superposition between i-th and j-th states.
Lastly, the time evolution of the density operator can be obtained from the Schrodinger equation for $|\psi_k\rangle$ and its dual bra:

$$\hat{H}|\psi_k(t)\rangle = i\hbar \frac{\partial |\psi_k(t)\rangle}{\partial t} \tag{40}$$

$$\langle \psi_k(t)|\hat{H} = -i\hbar \frac{\partial \langle \psi_k(t)|}{\partial t} \tag{41}$$

$$\frac{d}{dt}\rho(t) = \frac{d}{dt}\sum_k p_k[\frac{d}{dt}|\psi_k(t)\rangle\langle\psi_k(t)| + |\psi_k(t)\rangle\frac{d}{dt}\langle\psi_k(t)|] \tag{42}$$

obtaining the so called von Neuman equation:

$$\frac{d}{dt}\rho(t) = \frac{1}{i\hbar}[\hat{H}, \rho(t)]. \tag{43}$$

Commutation relation

The object appearing in the right hand side of Eq. (43) is a commutator. Given two operators $\hat{A}$ and $\hat{B}$ it is defined as:

$$[\hat{A}, \hat{B}] = \hat{A}\hat{B} - \hat{B}\hat{A}. \tag{44}$$

When the commutator between two operators is zero, the two are said to commute. It can be demonstrated that two commuting operators share a set of eigenstates. In physical terms, the observable associated to the operators can be observed simultaneously in a system's measurement. For example the position and momentum operators, $\hat{x}$ and $\hat{p} = i\hbar\frac{\partial}{\partial x}$ do not share any set of eigenstates, leading to a commutation relation: $[\hat{p}, \hat{x}] = i\hbar$. This result is well known in quantum mechanics e lead to the counter intuitive result that the position and momentum of a particle can never be observed by the same measurement.

$$\{\hat{A}, \hat{B}\} = \hat{A}\hat{B} + \hat{B}\hat{A}. \tag{45}$$

Reduced Density Matrix

As we have seen in section 2.2, entanglement is the result of the interaction between two systems. Often the two systems can be seen as environment and system of interest, the latter being the object of the observations. Environment is often inaccessible or not measurable, if not of no interest. Still, being entangled with the environment, the system is not describable with an individual state vector from which to derive its statistics. Let's consider an entangled state:

$$|w\rangle = \frac{1}{\sqrt{2}}(|e_1\rangle|s_1\rangle + |e_2\rangle|s_2\rangle). \tag{46}$$

Here $|e_i\rangle$ and $|s_i\rangle$, $i = 1, 2$, are normalized (but not necessarily orthogonal) states living in H_E and H_S respectively, Hilbert spaces associated to the environment and the system. Note that this is indeed a pure state, even though composite. Its density matrix will read:

$$\rho = |w\rangle\langle w| = \frac{1}{2}\sum_{i,j}|e_i\rangle\langle e_j| \otimes |s_i\rangle\langle s_j|. \tag{47}$$

Supposing now as observers to only have access trough measurements on the system's state. In other words consider now an operator acting only on the system S: $\hat{O} = \hat{O}_S \otimes \hat{I}_E$. Let's carry out the calculation of $\langle\hat{O}\rangle$, given and $|\phi_l\rangle$ $|\psi_k\rangle$ orthonormal bases of H_E and H_S :

$$\begin{aligned}
\langle\hat{O}\rangle &= Tr(\rho\hat{O}) && (48)\\
&= \sum_{k,l}\langle\phi_l|\langle\psi_k|\hat{\rho}(\hat{O}_S \otimes \hat{I}_E)|\phi_l\rangle|\psi_k\rangle && (49)\\
&= \sum_k\langle\psi_k|(\sum_l\langle\phi_l|\rho|\phi_l\rangle)\hat{O}_S|\psi_k\rangle && (50)\\
&= \sum_k\langle\psi_k|\rho_S\hat{O}_S|\psi_k\rangle && (51)\\
&= Tr_S(\rho_S\hat{O}_S). && (52)
\end{aligned}$$

Given the form of the operator, the trace on the environment was carried out immediately, yielding to the definition of a new operator, the reduced density matrix:

$$\rho_S = Tr_E\rho = \sum_l\langle\phi_l|\rho|\phi_l\rangle. \tag{53}$$

By tracing over the degrees of freedom of the environment of the system–environment density matrix, we obtained a mathematical object containing all measurement statistics that an observer can extract from the system. Note that reduced density matrix is necessarily non pure due to the presence of system–environment entanglement. Therefore, it is possible to compute the expectation value of an operator acting only on S as if the system were isolated and described by the reduced density matrix ρ.

2.4. Pauli Matrices

In order to discuss two level energy systems, we shall often use Pauli operators, first introduced to describe the spin state of the electron. Indeed, one of the most recurring configuration is that of a system effectively acting as a two-level system. This could happen for a system having discrete energy levels and interacting with an external perturbation, e.g. electromagnetic field, having an energy resonant with a couple of levels. The two levels can then in turn be mapped onto a two dimensional discrete Hilbert space, having a two vector orthonormal basis: $\{|0\rangle, |1\rangle\}$. In order to describe such two-level energy systems, Pauli operators were introduced. Consistently with the notation used so far, they would read:

$$\sigma_x \equiv |0\rangle\langle 1| + |1\rangle\langle 0|, \quad \sigma_y \equiv i|0\rangle\langle 1| - i|1\rangle\langle 0|, \quad \sigma_z \equiv |0\rangle\langle 0| - |1\rangle\langle 1|. \tag{54}$$

While in the much more common and handy matrix representation:

$$\sigma_x \equiv \begin{pmatrix} 0 & 1 \\ 1 & 0 \end{pmatrix}, \quad \sigma_y \equiv \begin{pmatrix} 0 & -i \\ i & 0 \end{pmatrix}, \quad \sigma_z \equiv \begin{pmatrix} 1 & 0 \\ 0 & 1 \end{pmatrix} \tag{55}$$

Being σ_z diagonal, the eigenstates correspond to the basis of the space:

$$|0\rangle = \begin{pmatrix} 1 \\ 0 \end{pmatrix}, \quad |1\rangle = \begin{pmatrix} 0 \\ 1 \end{pmatrix} \tag{56}$$

with eigenvalues $+1$ and -1.
Going further, it is possible to introduce the non hermitian lowering and raising operators:

$$\sigma_+ = |0\rangle\langle 1|, \quad \sigma_+ = \begin{pmatrix} 0 & 1 \\ 0 & 0 \end{pmatrix}, \tag{57}$$

$$\sigma_- = |1\rangle\langle 0|, \quad \sigma_- = \begin{pmatrix} 0 & 0 \\ 1 & 0 \end{pmatrix} \tag{58}$$

Even though they do not represent any observable, they act on the states allowing the transition from the lower to the higher and vice versa:

$$\sigma_+|0\rangle = 0, \quad \sigma_+|1\rangle = |0\rangle, \tag{59}$$

$$\sigma_-|1\rangle = 0, \quad \sigma_-|0\rangle = |1\rangle. \tag{60}$$

Note that Pauli operators can be rewritten as a suitable combination of σ_+ and σ_-. Also, any observable represented in this 2-dimensional Hilbert space can be rewritten as a suitable linear combination of the Identity matrix and the Pauli matrices.

2.5. Second quantization formalism

Trough this formalism it is possible to describe fields as operators, introducing the number state representation, and for that purpose it uses the destruction (annihilation) and creation operators. The quantization of electromagnetic field is a good example of how this formalism works [2]. Here we bring the example of the quatum harmonic oscillator as is a model that we used extensively in this work. First we recall the harmonic oscillator adimensional Hamiltonian:

$$\hat{H} = \frac{1}{2m\hbar\omega}[(m\omega\hat{x})^2 + \hat{p}^2] \tag{61}$$

where we have the operators associated to the canonically conjugated variables position $\hat{x}$ and momentum $\hat{p}$, m being the mass of the oscillator. We already briefly introduced annihilation and creation operator, but we did for a two dimensional Hermitian space, in matrix representation. In the Hilbert space defined by the oscillator system these operators read:

$$\hat{a}^\dagger = \frac{1}{\sqrt{2m\hbar\omega}}[m\omega\hat{x} + i\hat{p}] \tag{62}$$

$$\hat{a} = \frac{1}{\sqrt{2m\hbar\omega}}[m\omega\hat{x} - i\hat{p}] \tag{63}$$

one being the hermitian conjugated of the other, leading to the Hamiltonian to be reformulated:

$$\hat{H} = \hbar\omega(\frac{1}{2} + \hat{a}^\dagger\hat{a}) \tag{64}$$

The product between the operators appearing in this expression has a specific meaning and is called number operator $\hat{n} = \hat{a}^\dagger \hat{a}$. It clearly commute with the hamilotnian, with which it shares a set of eigenstates called the the number states $\{|n\rangle\}$ representing a complete and orthonormal basis. The eigenvalues of these states indicate the quanta of excitation of the oscillator. Starting from the so called zero point energy $\frac{\hbar\omega}{2}$, the energy separating each quantum is $\hbar\omega$. The creation and destruction operators act on these states respectively increasing and decreasing the value of the eigenvalue by one.

$$\hat{n}\hat{a}|n\rangle = (n-1)\hat{a}|n\rangle \quad (65)$$
$$\hat{n}\hat{a}^\dagger|n\rangle = (n+1)\hat{a}^\dagger|n\rangle. \quad (66)$$

It can be demonstrated that:

$$\hat{a}|n\rangle = \sqrt{n}|n-1\rangle \quad (67)$$
$$\hat{a}^\dagger = \sqrt{n+1}|n+1\rangle. \quad (68)$$

In the case of the electromagnetic field, the number states eigenvalues indicate the number of photon present for the mode identified by the frequency, and the number states are called Fock states. As a last remark, we highlight that these were the bosonic creation and annihilation operators. also fermions can be described in this type of formalism, with the creation and destruction operator having some different properties that we will later introduce.

3. Quantum Computing

The idea of encoding information in a quantum variable dates back to the 80s, and was first considered by Richard P. Feynman [3], and later postulated by D. Deutsch [4]. In its paper Deutsch had given an example of the superiority of quantum computing over classical deterministic computing. This superiority stems from three purely quantum properties:

- superposition: ability to be in multiple states at the same time,
- entanglement: ability to be part of one large quantum state together through entanglement,
- interference: exploiting quantum interference, see Eq. (16), it is possible to know the state of a quantum system without destroying it.

The single unit of information in quantum computing is called qubit, and it is in fact a quantum state. Due to superposition principle and entanglement, a quantum register composed by N qubits can be in a combination of 2^N number of states. On the contrary a classical register composed by N bits can be in one of the 2^N possible states. This is the difference at the core. Note that even if the quantum system is in superposition of states, once measured it will collapse in just one of them with a certain probability. As a matter of fact, no advantage can be taken from this configuration unless quantum interference is exploited before measuring the state of the system. Being all qubits entangled they will be described by an overall wavevector in a superposition of entangled state. This will set the probabilities of all the possible entangled state combinations through the coefficients. By changing the states of the qubits, i.e. manipulating them,probabilities can be changed and thus the outcome of any computation. In doing so constructive and destructive interference are exploited. The manipulation of these machines is in the realm of quantum algorithms. As a final remark, we point out that there are some problems that are thought to be intractable with classical computers while easily solvable with quantum computer: see Shor algorithm [5] for factorization. Furthermore, quantum encoding could yield a *physically* secure way of transmitting encoded information [6] due to the non cloning theorem [7]. Unfortunately, there are major obstacles in the implementation of this new technology, the main two being decoherence (i.e. entanglement with the environment) and noise, which will be the argument of section 3.2, both getting worst the more qubits are composing the system.

3.1. Quantum Bits

In classical computing the fundamental information unit, the bit, can take two possible values, 0 or 1. A quantum bit, also called qubit, is a two level quantum system, living in a two dimensional complex Hilbert space. The orthonormal basis set is formed by the vectors $|0\rangle$ and $|1\rangle$, which can be assigned to the classical bit states. In contrast with the classical bit, that can exist in one of the two, a qubit can be written as a superposition of these states:

$$|\psi\rangle = \alpha|0\rangle + \beta|1\rangle, \quad (69)$$

following Eq. (7). Also in this frame the normalization condition has to be satisfied with $|\alpha|^2 + |\beta|^2 = 1$. From what we have seen, it follows that a single qubit state is described by two real numbers, as opposed to the classical bit. In practice, a two level quantum system can be used as a qubit if:

- it can be prepared in a defined state,
- any state of the qubit can be transformed in any other state,
- it can be measured in the the basis $\{|0\rangle, |1\rangle\}$. The operator associated to this measurement is the Pauli matrix σ_z, whose eigenstates compose the basis, as per 2.4.

Representation: Bloch Sphere

Another way to rewrite the state $|\psi\rangle$ is:

$$|\psi\rangle = cos\frac{\theta}{2}|0\rangle + sin\frac{\theta}{2}e^{i\phi}|1\rangle. \tag{70}$$

Indeed, this expression respects the normalization requirements and we know that the overall phase factor can be neglected. This formulation allows us to visualize the state and its transformations in a geometric fashion. We can represent a single qubit state by a point on a sphere of unitary radius, called the Bloch sphere, Fig. 1. Coordinates of the point will be given by $x = cos\phi sen\theta, \quad y = sin\phi sin\theta, \quad z = cos\theta \quad$. When $\theta = 0$ the qubit state $|\psi\rangle$ will correspond to $|0\rangle$, while for $\theta = \pi$ $|\psi\rangle = |1\rangle$. Any other value of θ will correspond to a coherent superposition of states. From two measurements outcomes ± 1 associated to σ_z, corresponding to $|\psi\rangle = |0\rangle, |1\rangle$ can be obtained with probabilities:

$$|\langle 0|\psi\rangle|^2 = cos^2\frac{\theta}{2}, \quad |\langle 1|\psi\rangle|^2 = sin^2\frac{\theta}{2} \tag{71}$$

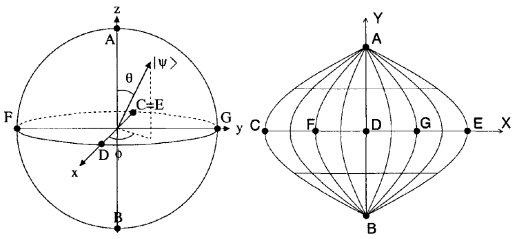

Figure 1: Bloch-sphere representation of a qubit (left) and sinusoidal projection of the Bloch sphere (right) from [8].

Measuring and manipulating the qubit

The measurement of a qubit will always give a projection of his quantum state over one of the two states composing thew basis, with a probability given by the coefficients α and β. Therefore no actual advantage is obtained solely from the coherent superposition of two states (or more in the case of quantum circuits). It is by exploiting quantum interference that the system can be put in a superposition with a higher probability of collapsing in the state encoding the information needed, when measured. In order to do so, depending on the type of computation, suitable algorithms have been invented to encode all the relevant information in the state with the highest probability. In other terms, constructive interference is used to increase the probability of collapse on the state with information, destructive interference is used to decrease the probability of collapse on the state with no or wrong information.
To implement the algorithms, as for classical computing, gates are used. In quantum computing the number of possible gates coincides with the number of possible unitary transformation of the qubit state, e.g. for a single qubit the infinite possible transformations that can be performed on the surface of the Bloch sphere. As said the only requirement is that the matrix associated to the transformation is unitary, being $\hat{M}$ the matrix:

$$\hat{M}\hat{M}^\dagger = \hat{I}. \tag{72}$$

Note that the matrix being unitary leads to the transformations being reversible as opposed to classical computations.
We shall now introduce some gates to clarify the type of actions performed on the qubit states.

Hadamard gate

Before going on let us introduce the column vector representation of a qubit:

$$|\psi\rangle = C_0|0\rangle + C_1|1\rangle = \begin{bmatrix} C_0 \\ C_1 \end{bmatrix} \tag{73}$$

In this notation every single-qubit gate will be a $2X2$ matrix. The Hadamard gate is defined as:

$$H = \frac{1}{\sqrt{2}} \begin{bmatrix} 1 & 1 \\ 1 & -1 \end{bmatrix}. \tag{74}$$

It acts on a generic state superposition as follows:

$$H|\psi\rangle = H \begin{bmatrix} C_0 \\ C_1 \end{bmatrix} = \frac{1}{\sqrt{2}} \begin{bmatrix} 1 & 1 \\ 1 & -1 \end{bmatrix} \begin{bmatrix} C_0 \\ C_1 \end{bmatrix} = \frac{1}{\sqrt{2}} \begin{bmatrix} 1 \\ 1 \end{bmatrix} = \frac{1}{\sqrt{2}} \begin{bmatrix} C_0 + C_1 \\ C_0 - C_1 \end{bmatrix} \tag{75}$$

Note that this gate turns the basis state $\{|0\rangle, |1\rangle\}$ in the following state superpositions:

$$H|0\rangle = \frac{1}{\sqrt{2}}(|0\rangle + |1\rangle) \tag{76}$$

$$H|1\rangle = \frac{1}{\sqrt{2}}(|0\rangle - |1\rangle) \tag{77}$$

Moreover, considering the fact that quantum gates are reversible:

$$H\frac{1}{\sqrt{2}}(|0\rangle + |1\rangle) = |0\rangle \tag{78}$$

$$H\frac{1}{\sqrt{2}}(|0\rangle - |1\rangle) = |1\rangle \tag{79}$$

Thus using this gate it is possible to prepare the initial state in a superposition of states, a key feature for quantum computing.

CNOT gate

As we have pointed out entanglement is the second key feature of quanutm computers. In order to have two entangled states a two qubit gate must be implemented, since it allows two qubit interactions. The gate allowing such to happen is the CNOT gate. Given two qubit as input, the gate will flip the second qubit (target) if the first (control) is in the state $|1\rangle$, and it will do nothing if the control is in state $|0\rangle$. The column vector representation of two entangled qubits reads:

$$|\psi\rangle = C_{00}|0\rangle|0\rangle + C_{01}|0\rangle|1\rangle + C_{10}|1\rangle|0\rangle + C_{11}|1\rangle|1\rangle = \begin{bmatrix} C_{00} \\ C_{01} \\ C_{10} \\ C_{11} \end{bmatrix} \tag{80}$$

Thus the gate in this case will be represented by a $4X4$ matrix:

$$U_{CNOT} = \begin{bmatrix} 1 & 0 & 0 & 0 \\ 0 & 1 & 0 & 0 \\ 0 & 0 & 0 & 1 \\ 0 & 0 & 1 & 0 \end{bmatrix}. \tag{81}$$

By applying this gate to a separable state we can see that it can be used to generate entangled states:

$$U_{CNOT}(\alpha|0\rangle + \beta|1\rangle)|0\rangle = \alpha|0\rangle|0\rangle + \beta|1\rangle|1\rangle \tag{82}$$

It can be demonstrated that a universal gate, i.e. a gate that allows arbitrary operations, can be implemented using single-qubit gates and CNOT gates [9].

3.2. Decoherence description: Master equations

At first we shall properly define decoherence. The interaction with the environment entails two main consequences for a quantum system, that we shall report as written in [10]:

1. The irreversible disappearance of quantum coherence, which as we have seen is responsible of state superposition and interference effects,
2. The definition of observable properties of the system, i.e. the selection of a set of preferred states.

In the following, when talking about decoherence, we will be referring to these two consequences, especially the first one. Quantum computing is indeed based on the superposition principle, and quantum computer is able to work as long as quantum coherence is preserved, therefore decoherence is a threat to the physical implementation. In this frame we point out that most of the research regarding the implementation of quantum computers is centred on the problem of controlling and minimizing decoherence. Even if at first one would be tempted to isolate as much as possible the qubits from the external world, it should be remembered that in a quantum computer a series of transformation and measurement shall be operated on the qubits, therefore they should remain accessible, at least up to a certain degree. The inner challenge in quantum computing is to address both these necessities, isolation and read out, finding the best trade off.
Decoherence dynamics can be described via the Master Equations. These equations describe the time evolution of the reduced density matrix $\rho_s(t)$ for a quantum system S interacting with the environment E. As we saw in Section 2.3, tracing out the degrees of freedom of the environment means not having to determine its dynamics. What is most interesting to us is indeed the influence of the environment on the system. In the master equation formalism, $\rho_s(t)$ is calculated from a first order differential equation of the form [10]:

$$\frac{d}{dt}\rho_S(t) = -\frac{i}{\hbar}[\hat{H}_S, \rho_S(t)] + \hat{D}[\rho_S(t)]. \tag{83}$$

The first term appearing on the right-hand side of the equation resembles to the term in the von-Neumann equation. However, $\hat{H}_S$ differs from the unperturbed Hamiltonian one of the system, as the influence of the environment causes a perturbation that leads to a re-normalization of the energy levels (assumed a weak interaction with the environment). The second and more interesting part shows a non-unitary operator representing Decoherence due to the environment. The derivation of this term won't be covered, we will only present the main approximation and their physical interpretation.

Approximations: Born-Markov master equation

Often it is impossible to determine the exact time evolution of $\rho_s(t)$. For this in the following we make use of these two approximations:

- Born Approximation: being the environment large with respect to the system, the interaction between the two does not lead to any significant changes of the density operator of the environment. In other words coupling between system and environment is sufficiently weak that they don't get entangled, i.e. the system-environment state can be described as an approximate product state.

$$\rho(t) \approx \rho_S(t) \otimes \rho_E \tag{84}$$

- Markov approximation: the self correlations within the environment due to coupling with the system decay faster than the characteristic timescale of the system dynamics. In other words, the environment is assumed being memory-less: the variation of ρ_E caused by the interaction have no effects on ρ_S. This is a non trivial requirement and it is not true in general [11].

Let's now assume the interaction Hamiltonian has the following form:

$$\hat{H}_{int} = \sum_\alpha \hat{S}_\alpha \otimes \hat{E}_\alpha, \tag{85}$$

where the operator $\hat{S}_\alpha$, assumed to be hermitian, correspond to physical quantities of the system that interact with the environment. We shall refer to them as being continuously monitored by the environment through the operator $\hat{E}_\alpha$. Given these assumptions and approximations, it can be demonstrated that the evolution of $\rho_S(t)$ is given by the Born-Markov master equation:

$$\frac{d}{dt}\rho_S(t) = -\frac{i}{\hbar}[\hat{H}_S, \rho_S(t)] - \sum_\alpha \{[\hat{S}_\alpha, \hat{B}_\alpha \rho_S(t)] + [\rho_S(t)\hat{C}_\alpha, \hat{S}_\alpha]\} \tag{86}$$

where:

$$\hat{B}_\alpha = \int_0^\infty d\tau \sum_\beta C_{\alpha\beta}(\tau)\hat{S}_\beta^{(I)}(-\tau), \quad \hat{C}_\alpha = \int_0^\infty d\tau \sum_\beta C_{\beta\alpha}(-\tau)\hat{S}_\beta^{(I)}(\tau) \tag{87}$$

Here $\hat{S}_\alpha^{(I)}(-\tau)$ stands for the system operator in the interaction picture, see section XX. $C_{\alpha\beta}(t)$ represent the environment self-correlation function:

$$C_{\alpha\beta}(\tau) = Tr_E \left\{ \hat{E}_\alpha(\tau)\hat{E}_\beta \rho_E \right\} = \langle \hat{E}_\alpha(\tau)\hat{E}_\beta \rangle_{\rho_E}. \tag{88}$$

This expression tell us to what extent he result of a measurement of a particular observable $\hat{E}_\alpha$ is correlated with the result of a measurement taken after a time τ. It quantifies to what degree the environment retains information over time about its interaction with the system. Given the Markov approximation these *correlators* are going to be sharply peaked around $\tau = 0$.
Even though at a first look this equation and its terms may be difficult to understand, it simplifies consistently in many case, such as situation in which just one operator of the system is monitored by the environment and for trivial time dependencies of the operators $\hat{S}_\alpha$ and $\hat{E}_\alpha$.

3.3. Physical Realisations and possible uses

As aforementioned, decoherence is the main threat to the practical realization of quantum computers. This is mainly due to the fact that when the scale of a quantum system increases, the coherence time, the time duration in which qubits can be manipulated, drops. In other words, the larger is the system the more likely it is to get entangled with the environment, loosing the information retained in the coherent superposition of system's states. As a result, it is very hard to realize a large scale quantum computer. For it to be achieved, decoherence timescale should be long with respect to the gate operation time. On the other hand, read-out of the state should be possible and reliable. In addiction, one should consider the preparation of the initial state and successive manipulation of it.
Therefore, we are facing conflicting objectives: a well isolated system with which we must strongly interact. In the following we will briefly introduce two examples of potential solutions to this problem. Both are examples of solid state qubits as this kind of frame display certain advantages: they are fabricated with established lithographic methods, allowing for scalability and tunability. Also, they show to be flexible in design and manipulation schemes, adding up to the fact that they can be easily embedded in electronic circuits. Lastly, the field of solid state physics and nanotechnologies is rapidly progressing. The main downturn is indeed the management of decoherence.

Superconducting qubits

One of the most popular approaches to encode qubits is based on superconductivity. Superconductors can support flowing charge currents without loss of energy, i.e. they have zero resistivity. In this type of material electrons form couples known as Cooper pairs. When a thin insulating barrier is put between two superconductors a Josephson junction is created. The cooper pairs can go through this junction via quantum tunneling, without any dissipation of energy. Cooper-pairs can be confined in boxes of micron size with electrostatic potentials. It is thus possible to use the two charge states of a box, differing by one cooper-pair, as the two states of a qubit. A cooper pair can move in and out the box via quantum tunneling and, by inducing oscillations between the two states, single qubit logic gates can be implemented. The maximum current flowing without destroying the junction is called critical current I_J, and is related to the Josephson energy $E_J = I_J\hbar/2e$. Depending on the ratio between this energy and the charging energy for a single cooper pair, three type of qubits can be defined: charge flux qubits, flux qubits and phase qubits. Qubit control has been demonstrated experimentally, making this proposed technology one of the most flexible in terms of different design types and manipulation. As a last remark, note that the operation of a two-qubit logic gate (CNOT), has been reported in recent years[12].

Spin qubits in quantum dots

Applying electrostatic potential to semiconductors, it is possible to deform the band structure of the electronic energy levels in order to create small three dimensional wells, of size comparable to the wavelength of the electrons. This confinement leads to the discretization of the energy levels [13], so that these potential confined regions, *dots*, can be regarded as macroscopic atoms. The interaction between two sufficiently close dots leads indeed to the formation of artificial molecules, via the overlapping of the electron wave funcitons of each dot. The number of electrons populating each dot can be controlled via the gate voltage applied to the semiconductor, down to just one electron. In this frame, the qubit can be realized through the spin state of a single electron quantum dot, $|0\rangle$ being spin up and $|1\rangle$ spin down. Inducing an energy gap between these two states via a magnetic field (effect known as Zeeman splitting), it is possible to control the qubit state with an oscillating magnetic field resonating with the splitting energy. In principle this type of scheme is scalable as, creating an array of so build qubits, they can be singularly adressed applying to each different gate voltages that would

in turn lead to different energy splitting due to the magnetic field. It is indeed possible to produce arrays of quantum dots with present technology [11].

We shall conclude this section pointing out that the effectiveness of each technology can be traced back to the trade-off problem between decoherence and controllability. It should be noted that current experiments have achieved coherent control of only a few qubits [14], the problem being that external control operations typically introduce noise into the qubit circuit, thus disturbing the programmed coherent evolution.

4. Device: Nano-mechanical qubit

Mechanical qubits have in recent years raised interest as an alternative to the already mentioned possible implementations of quantum computing. The reasons of interest are diverse. To begin with, a mechanical qubit could be sensitive to a wide range of force fields, since any force leads to a mechanical displacement [15]. Furthermore, these resonators can show large quality factors, leading to long coherence times[16] [17]. This would in turn allow to develop circuits with large number of qubits that still show long lasting coherence, as opposed to superconducting qubit circuits, where scale effect bring down the decoherence time with respect to a single qubit [18].
In order to make an oscillator suitable to be used as a qubit some sort of anharmonicity have to be introduced. The harmonic oscillator have indeed equal spaced energy levels, thus making it hard to access just two of them without interfering with others. The introduction of anharmonicity would generate a shift in the energy levels leading to energy-dependent spacing in the oscillator's quantized energy spectrum [19]. In this way controlled excitation of energy states (say the ground and first exited state) can be obtained which can be treated as a two level system (see Section 3.1).

4.1. Structure and Model

In order to obtain such a scheme, a suspended carbon nanotube has been proposed [20]. The idea is to couple the flexural modes of the nanotube to the charge state of an integrated double quantum dot obtained in the nanotube itself (Fig. 2). The double dot is formed using multiple gates generating an electrostatic potential along the nanotube. In this configuration therefore a double potential well is formed, each well having a set of discrete states. Here just two states, one for each well, are considered accessible, the others being at a higher energy due to Coulomb interaction. The Hamiltonian capturing this system is [20]:

$$\hat{H} = \frac{p^2}{2m} + \frac{m\omega_m^2 x^2}{2} + \frac{\epsilon}{2}\sigma_z + \frac{t}{2}\sigma_x - \hbar g \frac{x}{x_z}\sigma_z. \tag{89}$$

Here the first two term are those of the well known quantum harmonic oscillator [13], and refer to the flexural oscillation of the nanotube. The charge state in the double dot is here represented with Pauli matrices, with $\epsilon/2\sigma_z$ modelling the energy splitting and $t/2\sigma_x$ the interdot charge hopping trough tunneling, being $t/2$ the hopping energy term and ϵ is the energy difference between the two-dot states. The last term stands for the interaction between the charge state and the oscillator, where $\hbar g/x_z$ represents the variation in the force that acts on the oscillator, when the charge states varies. Here the zero point quantum fluctuation is introduced as $x_z = (\hbar/2m\omega_m)^{1/2}$. This last term is crucial as it conveys the interaction via the term g, a coupling constant that can be tuned acting on the gates creating the double dot structure.
We can first treat the system in a semiclassical approximated way in the Born-Oppenheimer picture: $\hbar\omega_m \ll \sqrt{t^2+\epsilon^2}$, therefore the displacement x is considered as a classical variable being the oscillation frequency very small w.r.t. other energies. From the diagonalization of the Hamiltonian given by Eq. (89), neglecting p^2, the two eigenvalues are obtained[20]:

$$\epsilon_\pm(x) = \frac{m\omega_m^2 x^2}{2} \pm \sqrt{\epsilon - (\epsilon - 2\hbar g x/x_z)^2 + t^2/2}. \tag{90}$$

This energy profile can be seen as the effective potential of the oscillator. The Taylor expansion for small x and $\epsilon = 0$ reads:

$$\epsilon_\pm(x) = \pm\frac{t}{2} + \frac{m\omega_m^2}{2}\left(1 \pm \frac{4\hbar g^2}{\omega_m t}\right)x^2 \mp \frac{4m^2\omega_m\hbar^2 g^4}{t^3}x^4 + ... \tag{91}$$

From this equation it can be easily seen how the coupling with the double dot lead to a variation of the quadratic coefficient, which is indeed $\propto \pm g^2$. Therefore the resonating frequency gets stiffened by the interaction for the upper branch, while softened for the lower branch. This is clearly depicted in Fig. 3. For $g = g_c^{sc} = (\omega_m t/4\hbar)^{1/2}$ the lower branch quadratic term is null and the potential is purely quartic: it is therefore expected that tuning g

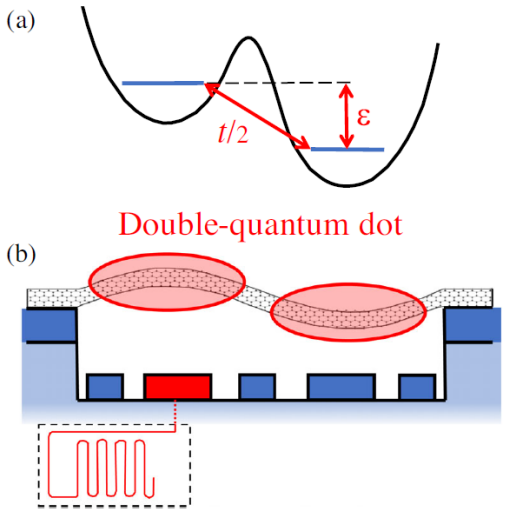

Figure 2: Schematic of the proposed setup. A suspended carbon nanotube hosting a double quantum dot, whose one-electron charged state is coupled to the second flexural mode. *a*. Sketch of the electronic confinement potential and of the two main parameters, the hopping amplitude t and the energy difference ϵ between the two single-charge states. *b*. Physical realization. One of the gate electrodes is connected to a microwave cavity for qubit readout.

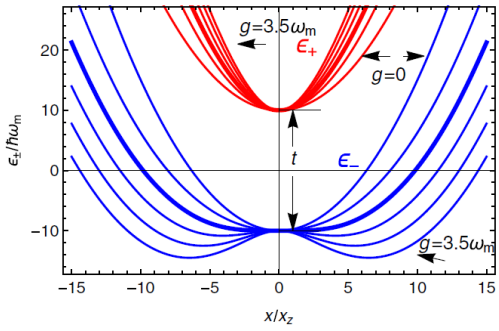

Figure 3: Effective potentials ϵ_+ and ϵ_-, for $t/\hbar\omega_m = 20$ and different values of $(4g/\omega_m)^2$. The thicker line corresponds to g_c^{sc}

around this value it should be possble to modify the ratio between the quadratic and quartic terms, controlling the degree of anharmonicity of the system. For even higher values of g Fig. 3 shows clearly the formation of a double well potential, i.e. a bistable configuration.

4.2. Implementing the qubit

Role of anharmonicity

Using a basis composed by the 10^2 lowest harmonic oscillator states it is possible to aproximately diagonalize the Hamiltonian from Eq. (89), so to finding the eigenvectors and eigenstates [20]. As already pointed out, the coupling constant g can be tuned by adjusting the gate voltages. Fig. 4 shows the dependence of the energy levels on g. It can be seen how the enhancement of the coupling leads to a separation of the third level $|2\rangle$ from the first two, $|0\rangle$ and $|1\rangle$, which for $g \gg g_c^{sc}$ would have the same energy. Defining the transition frequencies between two energy levels as:

$$\omega_{mn} = \frac{E_n - E_m}{\hbar}, \tag{92}$$

we can define the anharmonicity as:

$$a = \frac{\omega_{21} - \omega_{10}}{\omega_{10}}. \tag{93}$$

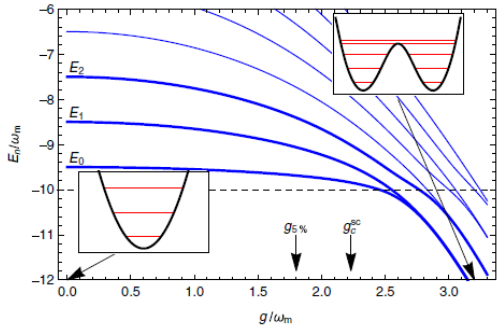

Figure 4: Lowest energy levels dependence on the coupling expressed as g/ω_m. The dashed line indicates the lowest non interacting electronic level $-t/2$.

Thus a will diverge for $g \gg g_c^{sc}$. As already pointed out, anharmonicity enables quantum control of the qubit effectively separating two levels from the others. Considering a value of a that allows this to happen, it has to be taken into account as a minimum requirement that the transition frequency ω_{10} between $|0\rangle$ and $|1\rangle$ needs to differ from ω_{12} between $|1\rangle$ and $|2\rangle$ by much more than the spectral line-width of the states.
Using as basis set the two qubit states $\{|0\rangle, |1\rangle\}$, the Pauli matrices $\{\tau_x, \tau_y, \tau_z\}$ and a unitary matrix τ_0 are defined. The notation is changed to distinguish from the Pauli matrices referring to the charge states. In this basis the Hamiltonian of the qubit is $\hat{H} = \hbar\omega_{10}\tau_z/2$. From the theory we know that every operator acting in this Hilbert space can be written as a linear combination of the four τ matrices. This is valid also for operators appearing in Eq. (89):

$$\sigma_x|_{qb} = \beta_1\tau_0 + \beta_2\tau_z \quad (94)$$
$$\sigma_y|_{qb} = \beta_3\tau_y \quad (95)$$
$$\sigma_z|_{qb} = \beta_4\tau_x \quad (96)$$
$$\hat{x}|_{qb} = \beta_5\tau_x \quad (97)$$
$$\hat{p}|_{qb} = \beta_6\tau_y. \quad (98)$$

Numerical methods can be implemented to obtain the coefficient β_i of the linear combinations describing the operators acting on the charge states σ_i, position $\hat{x}$ and momentum $\hat{p}$. In [20] analytical estimation of these coefficient where obtained. Among the many interesting features of these calculation, we shall highlight the fact that the projection of the charge operator σ_z in the qubit space, given by β_4, vanishes linearly for small g, remaining small for $g \leq \sqrt{\omega_m t/\hbar}$ if $t \gg \hbar\omega_m$. This meaning that the qubit has a predominantly mechanical character in its degrees of freedom, as the projection coefficients of $\hat{x}$ and $\hat{p}$, β_5 and β_6 respectively, remain in the order of the unity.

Decoherence

The nanomechanical qubit can be thought as being composed of two subsystems: the double quantum dot and the mechanical oscillator. Both these two are coupled with the environment, leading to decoherence. The subsystem having the larger decoherence rate, i.e. limiting the performances of the qubit, is the double quantum dot [21]. The Hamiltonian for the coupling with the environmet reads:

$$H_I = \hat{A}\hat{E}_1 + \hat{x}\hat{E}_2 \quad (99)$$

having $\hat{A} = \vec{v}\cdot\vec{\sigma}$ as the most general operator in the charge subspace. Note that here no coupling constants appear because they are absorbed in the $\hat{E}$ operators. In this frame, by tracing out the degrees of freedom of the environment, the reduced density matrix is obtained. Following the theory introduced in section 3.2, the study of ρ dynamics allows the description of decoherence in terms of the following rate equations for a two level system:

$$\dot{\rho}_{00} = \rho_{00}\Gamma_{01} + \rho_{11}\Gamma_{10}, \quad (100)$$
$$\dot{\rho}_{01} = -\rho_{01}(\Gamma_{01} + \Gamma_{10} + 2\Gamma_{01}^{\phi})/2, \quad (101)$$

where $\rho_{nm} = \langle n|\rho|m\rangle$ is the matrix element of ρ in the basis of the Hamiltonian Eq. (89). The terms Γ_{mn} are transition rates describing the probability of transition from one state $|n\rangle$ to another state $|m\rangle$ of the basis and

the term Γ_{01}^{ϕ} is the pure dephasing rate. Both these components are dependent on two quantities: the matrix elements of the operator $\hat{A}$ and the Fourier transform of the correlation function $C_i(t) = \langle \hat{E}_i(t)\hat{E}_i(0)\rangle$, defined as $S_i(\omega) = \int dt e^{i\omega t} C_i(t)$. Roughly speaking, in analogy with electronics, we could say that these functions $S_i(\omega)$ describe the energy spectrum of the noise generated from the interaction with the environment with the $i_t h$ subsystem.

$$\Gamma_{01} = 2\pi S_1(\omega_{01})|A_{01}|^2 + 2\pi S_2(\omega_{01})|x_{01}|^2, \tag{102}$$

$$\Gamma_{01}^{\phi} = \pi S_1(0)(A_{00} - A_{11})^2 + \pi S_2(0)(x_{00} - x_{11})^2. \tag{103}$$

As we have already mentioned in early chapters, the off-diagonal elements of a density matrix are called coherence elements, as their dynamic describe the ongoing coherent superposition in a system, at a given time. Eq. (101) is indeed very important, as it defines the coherence time of the qubit:

$$T_2 = \frac{2}{\Gamma_{01} + \Gamma_{10} + 2\Gamma_{01}^{\phi}}. \tag{104}$$

The study of this equation in the interacting case, i.e. $g \neq 0$ yields some notable results such as the fact that the pure dephasing rate is strongly reduced in the qubit compared to the charge system. Furthermore, also the decay rate gets dampened by the coupling represented by g. Lastly, the larger is t the larger the decoherence time, as a consequence from the mechanical nature of the qubit for $t > 2\hbar\omega_m$.

Manipulation

The coefficients describing the operators in the qubit basis are also crucial to understand the manipulation of the qubit. Control is implemented by an oscillating voltage applied to a wire near the nanotube, which couples to the charge state. In particular, this coupling can be studied through the coefficient associated to the interaction between the voltage and the operators σ_i and $\hat{x}$. Results from [20] find that standard methods such as nuclear magnetic resonance can be used to manipulate the qubit states.
In [22], readout was proposed exploiting the coupling of the system to a microwave superconducting cavity, similarly to what is done with superconducting qubits). In this work instead we investigated the possibility of reading out the states of the qubit through the capacitive coupling of its charge state with a nearby single electron transistor (SET). Hereafter we briefly introduce the main features of this device.

4.3. Read out device: Single electron transistor

Quantum tunneling and tunneling junction

Quantum tunneling is a purely quantum effect that is verified when a particle with an energy lower than a certain potential barrier crosses it due to non vanishing probability amplitude of the wavefunction beyond the barrier [13]. This effect has been largely observed and is exploited in technologies such as the scanning tunneling microscope. This effect is also exploited in electronics in the so called tunneling junction. This junction is composed by two metal leads (contacts) that are put in contact trough an insulating material, and is at the basis of the single electron transistor (SET). From a theoretical viewpoint, the electrons in the metals can be described as an ideal Fermi gas with a single particle dispersion $\epsilon = \hbar^2 k^2/2m$ with k the momentum of the particle and m its mass, disregarding the spin degree of freedom. In this description the tunneling can be seen as a perturbation in the Hamiltonian of the two leads Fermi gases. We introduce the resulting Hamiltonian as later will be largely used:

$$H = H_L + H_R + H_T \tag{105}$$

where $H_\alpha = \sum_k \xi_k c_{\alpha k}^\dagger c_{\alpha k}$ is the Hamiltonian of the Fermi gases, with $\alpha = R, L$ indicating left ad right lead, and $c_{\alpha k}$ fermionic destruction operator related to the electron occupation number states. Then we have the tunneling Hamiltonian $H_T = \sum_{k,k'} t_{kk'} c_{Lk}^\dagger c_{Rk'} + h.c.$. The general tunneling rate between two states i and f is given by the Fermi golden rule:

$$\Gamma_{i\to f} = \frac{2\pi}{\hbar}|M_{if}|^2 \delta(E_i - E_f) \tag{106}$$

Where M_{if} is the matrix element of the tunneling Hamiltonian, E_i and E_f are the energies of the initial and final state. The Dirac delta $\delta(E)$ accounts for energy conservation. While the previous formula holds for a single initial and final state, we have to deal with two Fermi gases, therefore the rate will depend also on the probability that initial state is occupied and that the final state isn't. In the case of non interacting fermions these probabilities are given by the energy dependent Fermi distribution functions $f_F(\epsilon) = 1/(1+e^{\epsilon/k_B T})$ where T is the temperature, and the Fermi energy is set to zero. When the two leads are connected to a voltage source,

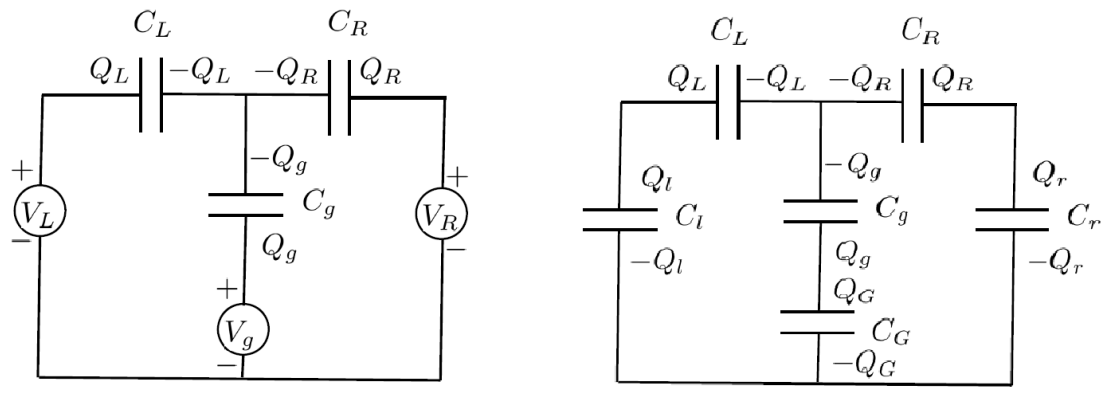

Figure 5: On the left: electrical scheme for the single electron transistor device. The central island is connected to the left and right leads by two tunnel junction here represented by two capacitance (C_L and C_R), and to a gate lead by a capacitance C_g. On the right: scheme for the single-electron transistor with the sources represented by capacitances, in practice a 5-metallic islands system is obtained

the difference in energy between the initial and final state (considering the battery as a large capacitance) is approximately $q_e V_b$, i.e. the value of the elementary charge times the bias voltage generated by the source. The resulting rate reads:

$$\Gamma_{L\to R} = \frac{2\pi}{\hbar} \sum_{kq} t_{kq}^2 f_L (1 - f_R) \delta(\epsilon_k - \epsilon_q + q_e V_b). \tag{107}$$

Via non trivial calculation considering the momenta as continuous variables, integrating and considering the fact that the density of state can be assumed constant near the Fermi level, the following is obtained:

$$\Gamma_{L\to R} = \frac{G_t}{q_e} \frac{V_b}{1 - e^{-q_e V_b / k_B T}}, \tag{108}$$

where we introduced the tunneling conductance $G_t = \frac{2\pi}{\hbar} \rho_L \rho_R |t|^2 q_e^2$.

Single electron transistor scheme

A single electron transistor (SET) is obtained when a micron-size metallic island is connected trough two tunneling junctions to two leads (source and drain) kept at voltages V_L and V_R by voltage sources. In addiction it has to be connected to a third conductor that acts as a gate, trough a capacitance C_g (Fig. 5, left). Considering all the voltage sources as ideal, the scheme of which in Fig. 5 (right) is obtained, where all the sources are substituted by capacitors, and now the structure can be thought as five metallic island connected trough capacitive coupling. In order to evaluate the tunneling rate toward the central micrometric island, the difference in the electrostatic energy when a charge is transferred from an island to another has to be evaluated. The computation of the energy difference between initial and final configuration when an electron tunnels is far from trivial. Here we report the main result:

$$\Delta E_{L,R}^{\pm} = E_C(Q \pm q) - E_C(Q) \pm q \sum_i \frac{V_i C_i}{C_\sigma} \mp q V_{L,R} \tag{109}$$

where coulomb energy defined as $E_C(Q) = \sum_i Q_i^2 / 2C_i$ and $C_\sigma = \sum_i C_i$ with i=L,R,g. Subscripts R and L indicate with which contact the charge exchange is taking place, and the superscript $\pm$ indicates whether the charge is being given of received from the metallic micrometric island. In order to determine the stable (no current flowing) and unstable (current flowing) configurations of this system one has to study the regions of V_g, V_L, V_R for which the energy variation are positive (stable) or negative (unstable).
This allows to identify the region where electron transport is possible, leading to the following expression for transition rates:

$$\Gamma_{L\to R}^{\pm} = \frac{G_t}{q_e} \frac{-\Delta E_{L,R}^{\pm}}{1 - e^{\Delta E_{L,R}^{\pm} / k_B T}}, \tag{110}$$

From Eq. (110) can be seen that the tunneling rate is strongly reduced for $\Delta E_{L,R}^{\pm} \gg k_B T$, increasing linearly for negative $\Delta E_{L,R}^{\pm}$.

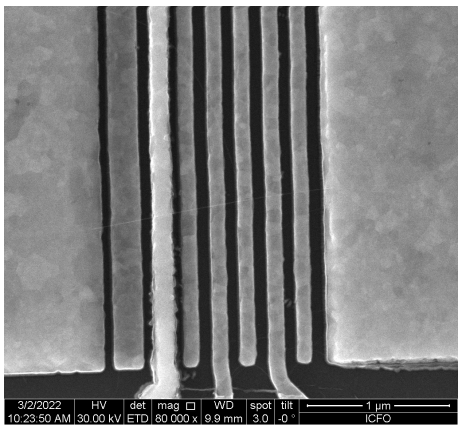

Figure 6: Device, courtesy A. Bachtold. In this picture, the thin line crossing the gates is the suspended carbon nanotube

If at low temperature gate and bias voltage are chosen in a way that $\Delta E_L^+ < 0$ and $\Delta E_R^- < 0$ only two rates are significantly different from zero $\Sigma_L^+ \equiv \Sigma_L$ and $\Sigma_R^- \equiv \Sigma_R$. This condition is called sequential tunneling, and it is indeed the condition in which the SET considered in this work is going to operate. Later on the master equation for the state of the central island are going to be written treating this condition in more depth.

5. A new idea for the read-out

In the paper in which the aforementioned structure was first proposed[20], read out and manipulation has been assumed possible using a microwave cavity coupled to the charge and to the displacement of the double quantum dot. In Fig. 6 a picture of one of the first samples fabricated by the group of A. Bachtold in 2022. In this work we aim to study a different way of detecting the displacement, or, more in general the nano-mechanical qubit (NMQbit). It is possible to fabricate a SET near the suspended carbon nanotube, and measure the current through the metallic island. Due to capacitive coupling between the charge in the metallic island and the charge in the double quantum dot, one can expect that the device could be very sensitive to any change in the charge of the double dot. Since the metallic island has nanometric size, in the following we are going to refer to it both as metallic island and single quantum dot. In addition, we note that we are going to assume the single quantum dot engineered (trough the gate voltage and the its dimensions) in a way that just one electron energy level is accessible, thus guaranteeing single electron passage. Since any displacement of the oscillator leads to a variation of the balance between the charge of the double quantum dot, one can detect in this way the displacement of the carbon nanotube. There are now several questions that we could ask. The first is of course which is the classical sensitivity of this detection. The second is how this method could be used to measure the qubit state, and finally what is the back-action on the coupled system oscillator-double quantum dot of the detection method. To answer these questions we begin by writing an Hamiltonian for the full system.

Hamiltonian

We can write the following Hamiltonian fro the full system:

$$H = H_S + H_T + H_{\mathcal{E}} + H_{S-\mathcal{E}} \tag{111}$$

Here H_S is the Hamiltonian of the system:

$$H_S = \epsilon_D \hat{n} - F_0 \hat{n}\hat{x} + g_c \hat{n}\sigma_z + \frac{\epsilon_{DD}}{2}\sigma_z + \frac{t}{2}\sigma_x + \hbar\omega_m a^\dagger a + g\sigma_z \hat{x} \tag{112}$$

where a is the destruction operator for the displacement of the mechanical oscillator, $\hat{x} = a + a^\dagger$, $\hat{n}$ the charge operator for the single dot (with eigenvalues 0 or 1), ϵ_D is the energy level of the metallic island (controlled mainly by the gate voltage), σ_z is the third Pauli matrix and represent the charge operator for the double dot, F_0 and g_c are the coupling of the charge state in the SET dot with the mechanical displacement and the charge of the single dot respectively. Lastly g is the coupling between the double dot and the displacement (see section 4.1). Note that the zero point energy of the oscillator has been here neglected. As for the other terms, H_T is

the Hamiltonian of Eq. (105),

$$H_T = \sum_{k,\alpha} \xi_{\alpha k} c_k^\dagger c_k + \sum_{kk'} \left[t_{kk'} c_{kL}^\dagger c_{k'R} + \text{h.c.} \right] \tag{113}$$

here $\alpha = L, R$ indicates the two leads coupled to the single dot, k is an eigenvalue used to lable the metallic lead electronic states of energy ξ_k, $T_{kk'}$ is the tunnelling amplitudes assumed constant.
The environment of the oscillator and the double dot is constituted mainly by the phonons in the carbon nanotube. This phonons can be thought to interact with the oscillator and the double dot separately, so to avoid many body problems. As a result the Hamiltonian both for the oscillator and for the double quantum dot is described as a collection of non interacting harmonic oscillators (corresponding to the phonons) thus the total energy being the sum of the parts. The coupling is assumed linear and given by the coupling constants n for the quantum dot and m for the oscillator. In the second quantization formalism the environment Hamiltonian will read:

$$H_{\mathcal{E}} = \sum_q \hbar\omega_q a_q^\dagger a_q + \sum_p \hbar\omega_p b_p^\dagger b_p, \tag{114}$$

while the interaction between the environment and the oscillator + double dot reads:

$$H_{S-\mathcal{E}} = \sigma \cdot \mathbf{n} \sum_q (a_q^\dagger + a_q) + \hat{x} \sum_p c_k (b_p^\dagger + b_p). \tag{115}$$

5.1. SET Back action on the oscillator

Following our purpose of evaluating the back-action of the detection method on the qubit, we start by considering the coupling between the quantum dot and the oscillator. We hereby define the Hamiltonian of the oscillator-quantum dot system re-arranging some of the already encountered terms:

$$H = H_O + H_D^{'} + H_T, \tag{116}$$

where H_T is the previously defined tunneling Hamiltonian, $H_O = \hbar\omega_m a^\dagger a$ is the oscillator Hamiltonian and

$$H_D^{'} = \epsilon_D \hat{n} - F_0 \hat{n} \hat{x} \tag{117}$$

is the quantum dot Hamiltonian, in which the second term on the right-hand side is the term due to the coupling between the oscillator and the dot.
In the following we treat the oscillator classically, considering the tunneling rates much higher then the oscillator frequency, $k_B T/\hbar \gg \Gamma \gg \omega_m$, since this is a common experimental case. In this way we can give an exact description of the oscillator motion. This said the energy level in the dot will be:

$$\epsilon_D' = \epsilon_D - F_0 \langle \hat{x} \rangle. \tag{118}$$

The motion of the oscillator thus provokes a change in the dot energy level, perturbing it. The force operator that drives the interaction is

$$\hat{F} = -\frac{\partial H_D^{'}(x)}{\partial x} = F_0 \hat{n} \tag{119}$$

In the following we will derive the dot's energy level dependence of the SET's tunneling rates.

Oscillator response

The interaction Hamiltonian between the oscillator and the charge state of the SET island capacitively coupled with it reads:

$$H_{int} = -F_0 \hat{n} x. \tag{120}$$

When the oscillator is assumed coupled to the SET and to a bath of oscillators (i.e. the phonons). The motion can be described by a classical Langevin equation [23]:

$$m\ddot{x} = -kx - m\gamma_0 \dot{x} + f_0 + F_0 n(t), \tag{121}$$

where $f_0 - m\gamma_0 \dot{x}$ are the environment induced terms, with γ_0 the damping and f_0 the corresponding fluctuating force. The remaining part $F_0 n(t)$ is the term describing the back action of the quantum dot on the oscillator, with $\hat{n}$ standing for the occupation state of the dot. Both the environmental-due force and the charge back

action have fluctuating components. Indeed, $F_0 n(t)$ can be described as the sum of a fluctuating part and an average part. In order to evaluate the noise induced on the oscillator by the conductor (i.e. the dot of the SET) we are going to evaluate the effective temperature caused by their interaction. To do so we have to introduce the results of the quantum linear response theory [24], in terms of two main factors: fluctuation and damping. We define the quantum noise spectrum associated to a quantum operator, in this case the charge state in the quantum dot $\hat{n}$ that, from now on, we are going to indicate as n:

$$S_n(\omega) = \int_{-\infty}^{+\infty} \langle n(t)n(0)\rangle e^{-i\omega t} dt. \tag{122}$$

We note that quantum noise is defined similarly to classical noise, although it can be demonstrated not being symmetric. Just to give a scent of what this means it can be said that the positive-frequency part of the spectral density is a measure of the ability of the oscillator to absorb energy, while the negative-frequency part is a measure of the ability of the oscillator to emit energy. This is the term from which we are going to retrieve both the fluctuation magnitude and the damping:

$$\gamma(\omega) = \frac{F_0^2}{m}\left(\frac{S_n(\omega) - S_n(-\omega)}{\omega}\right). \tag{123}$$

This last result of quantum linear response theory that we are taking for granted is the so called fluctuation-dissipation relation, stating that noise and damping are related to one another via the temperature, specifically it links the classical symmetric-in-frequency part of the noise to the damping. Introducing the symmetrized quantum noise of the operator $\hat{n}$.

$$\overline{S_n} = \frac{F_0^2}{2}[S_n(\omega) + S_n(-\omega)] = \frac{1}{2}\coth\left(\frac{\hbar\omega}{2k_B T_{eff}(\omega)}\right)(S_n(\omega) - S_n(-\omega)) \tag{124}$$

Putting together Eq. (124) and Eq. (123)it we obtain:

$$\coth\left(\frac{\hbar\omega}{2k_B T_{eff}(\omega)}\right) = \frac{\overline{S_n}(\omega)}{m\gamma\hbar\omega}, \tag{125}$$

Going on we can consider the oscillator frequency ω small compared to the tunneling rates Γ. This is usually true since ω is usually in the order of 100 MHz, producing a very small current in the order of $\omega e = 10^{-11}A$. In this regime we can try to give an exact description of the oscillator dynamics, thanks to the separation of time scales.
In this case the effective temperature can be obtained from the equation:

$$k_B T_{eff} = \frac{F_0^2 S_n(0)}{2m\gamma}. \tag{126}$$

The effective temperature indicates the amount of excitement induced in the oscillator by the interaction with the metallic island charge state, thus being a measure of the induced noise in the oscillation.

SET rates

Considering the tunneling from a metal to a Quantum dot described by a single level that can be either occupied or not, the suitable expression for the tunneling rate is the following:

$$\Gamma^+_{L,R} = \frac{2\pi}{\hbar}\sum_f |M_{if}|^2 P_i \delta(E_i - E_f) \tag{127}$$

where P_i is the probability of the initial state in the metal of being occupied and the sum is operated over all the final states. The sum can be performed via an integral changing the variable to energy and using the density of states, which we are going to assume constant given that the transport properties are mainly influenced by electrons at the Fermi level. Using the results of appendix A we obtain:

$$\Gamma^+_L = \frac{2\pi}{\hbar}\rho|M|^2 f_F[\epsilon_1 - ec_g(V_g - V_L) - ec_R(V_R - V_L)], \tag{128}$$

$$\Gamma^+_R = \frac{2\pi}{\hbar}\rho|M|^2 f_F[\epsilon_1 - ec_g(V_g - V_R) - ec_L(V_L - V_R)] \tag{129}$$

where $\epsilon_1 = \epsilon_D^{'} + \frac{e^2 - 2Qe}{2C_\Sigma}$ and $\epsilon_D^{'} = \epsilon_D - F_0\langle\hat{x}\rangle$ as we wrote

$$E_i = \epsilon_k + E_i^C, \qquad E_f = \epsilon_D^{'} + E_f^C. \tag{130}$$

With E^C coulomb energy of the SET. We thus obtained the dependence of $\Gamma^+_{L,R}$ on the movement of the oscillator. According to appendix A, we can write the rates in a more compact form, for both the tunneling towards the dot and from the dot to the leads:

$$\Gamma^+_L = \Gamma^0_L f_L, \qquad \Gamma^+_R = \Gamma^0_R f_R \tag{131}$$

where

$$f_L(\epsilon^{'}_D) = f_F[\epsilon_1 - ec_g(V_g - V_L) - ec_R(V_R - V_L)], \tag{132}$$
$$f_R(\epsilon^{'}_D) = f_F[\epsilon_1 - ec_g(V_g - V_R) - ec_L(V_L - V_R)] \tag{133}$$

and, considering the reverse process:

$$\Gamma^-_L = \Gamma^0_L(1 - f_L), \qquad \Gamma^-_R = \Gamma^0_R(1 - f_R). \tag{134}$$

In the following we are going to refer to the total + or - rates, respectively:

$$\Gamma^+ = \Gamma^+_L + \Gamma^+_R, \tag{135}$$
$$\Gamma^- = \Gamma^-_L + \Gamma^-_R. \tag{136}$$

Quantum dot charge power spectrum

We consider the island charge n as fluctuating between the values 0 and 1, with occupancy time of the island determined by the rates Γ^+ and Γ^-. Note that we are interested in the fluctuating part of the noise spectrum, thus we evaluate $\langle \tilde{n}(t)\tilde{n}(0)\rangle = \langle n(t)n(0)\rangle - \overline{n}^2$. To do such a thing we take into account the master equations for the charge state of the island, describing the probabilities P_1, island occupied by the charge, and P_0 island unoccupied.

$$\dot{P}_0 = -\Gamma^+ P_0 + \Gamma^- P_1, \tag{137}$$
$$\dot{P}_1 = -\Gamma^- P_1 + \Gamma^+ P_0. \tag{138}$$

The solution of the system gives

$$P_1 = P_1(0) + [P_{st} - P_1(0)](1 - e^{-t\Gamma_\Sigma}). \tag{139}$$

Here $\Gamma_\Sigma = \Gamma^+ + \Gamma^-$ is the total tunneling rate, $P_{st} = \frac{\Gamma^+}{\Gamma_\Sigma}$ is the stationary solution leading the mean value of the charge to correspond to $\overline{n} = eP_{st}$. Moreover the stationary current is defined as $I = \frac{e\Gamma^+\Gamma^-}{\Gamma^+ + \Gamma^-}$.
Back to the noise spectrum, we need to evaluate

$$\langle n(t)n(0)\rangle = P_1|_{P_1(0)=1} P_{st} \tag{140}$$

in order to compute

$$\tilde{S}_n(\omega) = \int_{-\infty}^{+\infty} [\langle n(t)n(0)\rangle - \overline{n}^2] e^{-i\omega t} dt. \tag{141}$$

Considering the island occupied at zero time, $P_1(0) = 1$ we are left with the calculation of a Fourier transform, that eventually lead us to

$$S_n(\omega) = \frac{2\overline{\Gamma}}{\Gamma^2_\Sigma + \omega^2}, \tag{142}$$

where $\overline{\Gamma} = \frac{\Gamma^+\Gamma^-}{\Gamma_\Sigma}$. Furthermore since we're considering the oscillator frequency to be small compared to tunneling rates, $\omega \to 0$ we'll have

$$S_n(\omega) \to \frac{2\Gamma^+\Gamma^-}{\Gamma^3_\Sigma}. \tag{143}$$

This is the final expression for the noise induced fluctuations, generated by the charge state and affecting the oscillator.
The previous master equations also allows us to evaluate the damping term, relating it to the tunneling rates. Given that $P_1 = 1 - P_0$, from Eq. (137) and Eq. (138) we obtain the following expression:

$$\dot{P}_1 = -\Gamma_\Sigma P_1 + \Gamma^+ \tag{144}$$

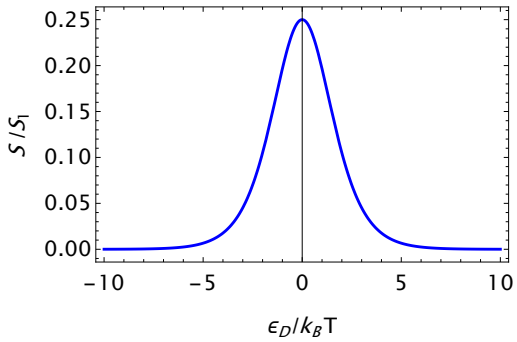

Figure 7: Fluctuations for equilibrium conditions

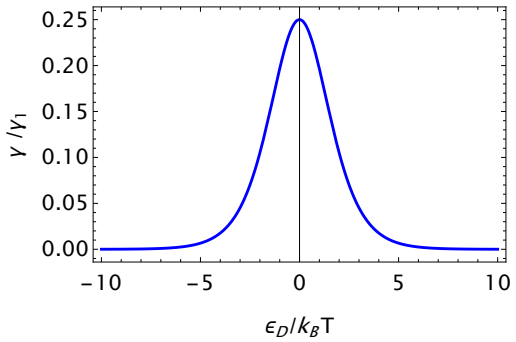

Figure 8: Damping for equilibrium conditions

which we expand in subsequent order terms:

$$\dot{P}_1^{(0)} + \dot{P}_1^{(1)} = -\Gamma_\Sigma(P_1^{(0)} + P_1^{(1)}) + \Gamma^+ \tag{145}$$

equating the same order terms we obtain the expression for the stationary solution and for the first order correction:

$$P_1^{(0)} = \frac{\Gamma^+}{\Gamma_\Sigma}, \tag{146}$$

$$P_1^{(1)} = -\frac{1}{\Gamma_\Sigma}\frac{\partial}{\partial x}\frac{\Gamma^+}{\Gamma_\Sigma}\dot{x}. \tag{147}$$

If we consider the general relation between energy and force:

$$\frac{\partial}{\partial x}E = -F_0, \tag{148}$$

with E energy of the quantum dot, we obtain the first order correction to the force:

$$P_1^{(1)}F_0 = \frac{F_0^2}{\Gamma_\Sigma}\frac{\partial}{\partial E}\frac{\Gamma^+}{\Gamma_\Sigma}\dot{x} \tag{149}$$

from which we can extract the expression for the damping term:

$$m\gamma = -F_0^2\frac{\partial_E(\Gamma^+/\Gamma)}{\Gamma_\Sigma}. \tag{150}$$

We assume that $\Gamma = \Gamma^+ + \Gamma^- = \Gamma_L^0 + \Gamma_R^0$, a constant, thus we obtain:

$$m\gamma = -F_0^2\frac{\partial_E(\Gamma^+)}{\Gamma_\Sigma^2}. \tag{151}$$

We will these expressions to advance some considerations about the behaviour of the damping term and the fluctuating term over energy. Eventually we'll do the same for the effective temperature, which expression in light of Eq. (126), Eq. (143) and Eq. (151) is:

$$k_B T_{eff} = -\frac{\Gamma^+\Gamma^-}{\Gamma_\Sigma\partial_E(\Gamma^+)}. \tag{152}$$

Equilibrium

At equilibrium, i.e. assuming the two leads to be at the same voltage, $f_L = f_R = f$, we obtained the following expressions:

$$\gamma = \frac{F_0^2}{\Gamma_\Sigma m k_B T}f(1-f) = \gamma_1 f(1-f) \tag{153}$$

$$S_n = \frac{2F_0^2}{\Gamma_\Sigma}f(1-f) = 2S_1 f(1-f) \tag{154}$$

$$T_{eff} = T \tag{155}$$

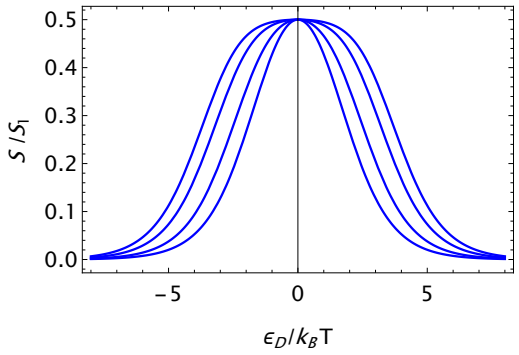

Figure 9: Fluctuations for $V_1 = 2, 3.5, 5, 6$

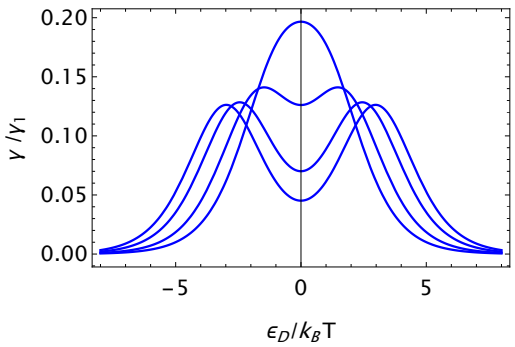

Figure 10: Damping for $V_1 = 2, 3.5, 5, 6$

Where we used the derivative $f' = \frac{f(f-1)}{k_B T}$. Substituting back the Fermi distribution we have explicit energy dependencies for these quantities (Fig. 7, Fig. 8). We note that both for the fluctuations and for the damping when the energy of the quantum dot level coincides with the Fermi energy level of the two leads, i.e. when the tunneling event are maximized, we reach the maximum value. In Fig. 7 and Fig. 8 the zero of energy coincides with the Fermi level of the leads. The effective temperature is always constant and coincides with the temperature T.
For simplicity and being it possible to implement experimentally, in the following Γ_L^0 and Γ_R^0 will be considered equal.

Out of equilibrium

The difference in voltage will cause different distribution in the two leads.Given V the voltage difference, the energy difference between the two Fermi levels will be $-eV$. Functions as plotted are dependent on energy of the dot normalized on the thermal energy and the parameter $V_1 = eV/k_B T$ Assuming the right lead to be at higher voltage than the left lead, Fermi distributions will read:

$$f_R(\epsilon_D, V) = \frac{1}{e^{\beta(\epsilon_D + eV/2)} + 1} = \frac{1}{e^R + 1} \tag{156}$$

$$f_L(\epsilon_D, V) = \frac{1}{e^{\beta(\epsilon_D - eV/2)} + 1} = \frac{1}{e^L + 1} \tag{157}$$

where we put the zero of the energy in correspondence of the unbiased Fermi energy for the leads. We recall that $\Gamma_L^0 = \Gamma_R^0 = \Gamma$. We therefore proceed to evaluate again the expressions for damping, fluctuations and effective temperature:

$$\gamma = \frac{F_0^2}{4\Gamma m k_B T}(f_L(1-f_L) + f_R(1-f_R)) = \frac{\gamma_1}{2}(f_L(1-f_L) + f_R(1-f_R)), \tag{158}$$

$$S_F = \frac{F_0^2}{4\Gamma}(f_L + f_R)(2 - f_L - f_R) = \frac{S_1}{2}(f_L + f_R)(2 - f_L - f_R), \tag{159}$$

$$\frac{T_{eff}}{T} = 1 + \frac{1}{2}\frac{(f_L - f_R)^2}{f_L + f_R - f_L^2 - f_R^2}. \tag{160}$$

From these expression we obtain the dependence on these quantities on the quantum dot energy level position and the voltage bias applied. It's immediate to see that:

$$\gamma \propto -(f_L' + f_R') \tag{161}$$

Therefore the damping will be characterized by two peaks coinciding with the Fermi levels of the two metal leads, i.e. when at $\epsilon_D = \pm eV/2$, displaying a local minimum for $\epsilon_D = 0$. Both damping and fluctuations go to zero for $|\epsilon_D| >> eV/2$. One should notice that the fluctuations maximum value does not depend on the bias voltage applied, while the FWHM is eV (Fig. 9). The function increases like $1 - (f_R)^2$ for $\epsilon_D \to -(eV/2)^-$ and decreases like $f_L(2 - f_L)$ for $\epsilon_D \to (eV/2)^+$. Near the zero this term increases more or less slowly depending on V, reaching the maximum for $\epsilon_D = 0$. The effective temperature (Fig. 11) starts from the limiting value of T and reaches a maximum for $\epsilon_D = 0$ showing exponential behaviour around $\pm eV/2$. We underline that the dependence of the effective temperature on the voltage has an exponential nature, therefore in experiments one would want to limit the bias. For $eV > k_B T$ the effective temperature rapidly increases reaching high value

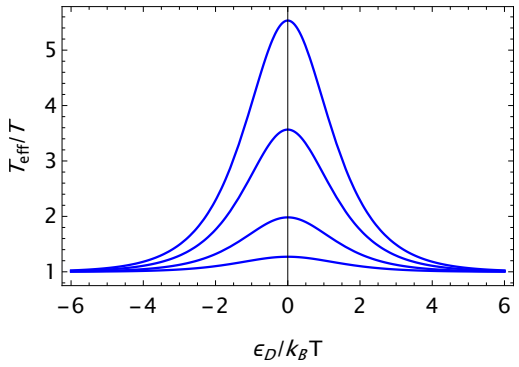

Figure 11: T_{eff}/T lineshape broadening and increasing with the voltage. Here represented for $V_1 = 2, 3.5, 5, 6$.

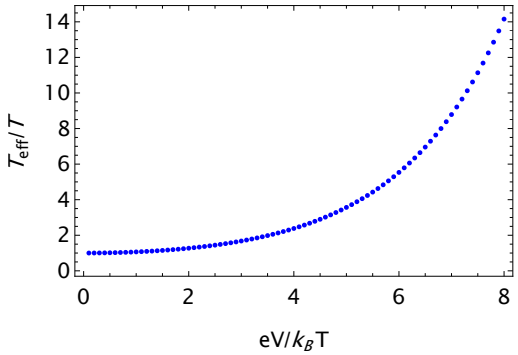

Figure 12: Exponential dependence of the Max of T_{eff}/T on the voltage bias, displayed for $V_1 = 0$ to 8 with a 0.1 step

at its maximum, since for energy among zero the damping term reaches very low values, Fig. 10, while the fluctuation for $\epsilon_D = 0$ is constant. We recall that the temperature of the oscillator is given by both the effects of the environment and the quantum dot, Eq. (121). In this section we neglected the effects of the bath of oscillator, whose effects could be explored in further studies.

5.2. Double Dot effects on response to back-action

In this section we are going to investigate the effects of the coupling between the double dot and the oscillator on the back-action of the Detection method on the oscillator, consistently with the semiclassical treatment. The oscillator and Double Dot Hamiltonian reads:

$$H = \frac{p^2}{2m} + \frac{m\omega_0^2}{2}x^2 + \frac{t}{2}\sigma_x + (\frac{\epsilon_{DD}}{2} + gx)\sigma_z. \tag{162}$$

Once the double dot Hamiltonian is diagonalized, it all can be rewritten as:

$$H_{DD} = \left(\frac{1}{2}\sqrt{(\epsilon_{DD} + 2gx)^2 + t^2}\right)\sigma_z. \tag{163}$$

In the following we will consider $\epsilon_{DD} = 0$ since it is the most relevant case in terms of sensitivity. As a consequence of the presence of the double dot therefore the total energy of the oscillator-double dot system splits in two branches:

$$E^{\pm} = \frac{m\omega_0^2}{2}x^2 \pm \frac{1}{2}\sqrt{(2gx)^2 + t^2}, \tag{164}$$

where we neglected the kinetic energy term. For small displacements, we can expand in series this expression, stopping at the second order:

$$E^{\pm} = \frac{m\omega_0^2}{2}x^2 \pm \left(\frac{t}{2} + \frac{g^2x^2}{t}\right) \tag{165}$$

or, in a better fashion:

$$E^{\pm} = \left(\omega_0^2 \pm \frac{2g^2}{mt}\right)\frac{m}{2}x^2 \pm \frac{t}{2}. \tag{166}$$

Each energy branch will correspond to a different state of the two level system set up by the double dot and oscillator. Each branch will have a different resonating frequency:

$$\omega^{\pm} = \left(\omega_0^2 \pm \frac{2g^2}{mt}\right)^{1/2}. \tag{167}$$

We note that for high values of t, even if the splitting between the branches increases, the difference in the quadratic coefficients is very small, meaning that the two branches are characterized by almost the same resonant frequency. Given the assumption made in Section 5.1, i.e. oscillator frequency much smaller than tunneling rates, the damping coefficient does not depend on frequency, see Eq. (151), therefore at first order no variation in behaviour is expected even when considering the double quantum dot effects. In principle fluctuations should be dampened by higher values of resonant frequency, stiffened by the interaction with the double dot for the

lower branch, and enhanced by lower values of the resonant frequency in the lower branch. On the other hand in Eq. (143) the assumption of oscillating frequency being small with respect to the tunneling rates leads again to a non dependence on the frequency. This allow us to say that at first order the double dot does not change the behaviour of the back action when considered.

6. Device sensitivity to displacement

6.1. Semiclassical approach

We aim to retrieve a relation between the current and the displacement, given that the current will be a function of the energy level in the dot ϵ_D and the bias voltage between the two metals. In turn, the energy of the dot will be affected by the displacement on the oscillator as we already know from section 5.1. We assume the device to be working in sequential tunneling regime, $k_BT/\hbar \gg \Gamma_\alpha$, where T is the temperature and Γ_α are the tunneling rates for the double quantum dot. Since $k_BT/\hbar \gg \Gamma \gg \omega_m$ this approach is valid only in the classical limit of the mechanical oscillator. This being said we can express the operators acting on the oscillator subspace as their quantum averages:

$$\epsilon_D \to \epsilon_D = \epsilon_D + g_c\langle\sigma_z\rangle - F_0\langle\hat{x}\rangle. \tag{168}$$

As already done we diagonalize the Hamiltonian of the double dot

$$H_{DD} = \left(\frac{\epsilon_{DD}}{2} + gx\right)\sigma_z + \frac{t}{2}\sigma_x = \frac{1}{2}\begin{pmatrix} \epsilon_{DD}+2gx & t \\ t & -\epsilon_{DD}-2gx \end{pmatrix} \tag{169}$$

obtaining: $U^\dagger H_{DD} U = \sigma_z E_{DD}(x)/2$ with

$$E_{DD} = \sqrt{(\epsilon_{DD}+2gx)^2 + t^2} \tag{170}$$

and $U = e^{-i\theta\sigma_y/2}$ with $\tan\theta = t/(\epsilon_{DD}+2gx)$. Assuming the system in the ground state we calculate the change in the charge unbalance as a function of the displacement:

$$\langle\sigma_z\rangle = \langle U^\dagger\sigma_z U\rangle = -\cos\theta = -\frac{(\epsilon_{DD}+2gx)}{\sqrt{(\epsilon_{DD}+2gx)^2+t^2}}. \tag{171}$$

Expanding in series for small displacements and putting everything in Eq. (168) we get for ϵ_D:

$$\epsilon_D = \epsilon_D^0 + \left[-\frac{2t^2 g g_c}{(\epsilon_{DD}^2+t^2)^{3/2}} + g_x\right]\hat{x} \tag{172}$$

where we included into ϵ_D^0 the first term of the expansion. In particular we know that $\epsilon_D \propto (C_g/C_\Sigma)eV_g$, thus if we know the current dependence on V_g we can derive the current dependence on any displacement. Note that in Eq. (172) we are indicating the dimensionless displacement by $\hat{x} = a + a^\dagger$, the dimensionfull being $x = x_{\text{zpm}}\hat{x}$ with $x_{\text{zpm}} = \sqrt{\hbar/2m\omega_m}$ and m the mass of the oscillator. By equating the two expressions for ϵ_D and exploiting the chain rule we get the derivative of the current with respect to the oscillator displacement, in which the dependence of the current on the gate voltage is assumed known:

$$\frac{dI}{dx} \propto \frac{C_\Sigma}{C_g e}\frac{dI}{dV_g}\frac{1}{x_{\text{zpm}}}\left[-\frac{2t^2\hbar^2 g g_c}{(\epsilon_{DD}^2+t^2)^{3/2}} + g_x\right] \tag{173}$$

We can see that the first term in the square brakets is maximum for $\epsilon_{DD} = 0$ giving

$$\left.\frac{dI}{dx}\right|_{\max} \propto -\frac{dI}{dV_g}\frac{C_\Sigma}{C_g e}2\frac{\hbar g_c}{t}\frac{\hbar g}{x_{\text{zpm}}} \tag{174}$$

Note that the last term represents the variation of the force on the nanotube when an electron is displaced from the left to the right dot. Note that the calculation holds for $k_BT \ll \sqrt{\epsilon_{DD}^2+t^2}$, otherwise we cannot assume anymore that the electronic system is in the ground state. If we include the upper state in the average we obtain the following expression for the maximum sensitivity, which resembles the former:

$$\left.\frac{dI}{dx}\right|_{\max} \propto -\frac{dI}{dV_g}\frac{C_\Sigma}{C_g e}2\frac{\hbar g_c}{t}F_0\tanh(t/2k_BT). \tag{175}$$

From this is clear that decreasing t the sensitivity grows. In more physical terms, the easier is for the charge to hop from one dot to the other, via tunneling effect, the more amplified is the sensitivity to the motion of

the oscillator, since the coulomb interaction between the charge state in the double dot and in the SET is what drives the device. If we consider the case for which $t \ll k_B T$ one obtains:

$$\left.\frac{dI}{dx}\right|_{\max} \propto -\frac{dI}{dV_g}\frac{C_\Sigma}{C_g e}\frac{\hbar g_c}{k_B T}F_0 \tag{176}$$

For a rough estimation of g_c, the coupling constant representing the capacitive coupling between the double dot and the dot one can consider the term $\frac{\hbar g_c}{k_B T}$. This terms tell us that in order to have a gain in sensitivity the capacitive coupling should be larger than the temperature. If the temperature is 10 mK this implies $g_c > 10$ GHz. Being this a coupling between charge states this condition is achievable, even if it's very strong. In [25] a quantum dot has been used to detect a double quantum dot, finding that the conductance in units of the quantum of conductance changes from 0.1 to 0.3 corresponding to a variation of the gate voltage of the dot of 10 mV. Therefore large values of the coupling constant may be achievable also in the proposed structure. The additional advantage of this method is that it does not require a current to flow through the double quantum do to measure the displacement of the oscillator. It is thus expected that the back-action on the oscillator can be smaller. The method exploits the fact that a small change in the displacement induces a large change in the charge of the dot. The double quantum dot acts as a quantum amplifier. It may be difficult to tune the parameters in such a way that the tunnelling rate is smaller than the temperature, then the same expression holds with t replacing $k_B T$. Still a large effects possible.

6.2. Full quantum description of sensitivity

Let us now consider the problem without the assumption of semiclassical behavior. Furthermore let's formulate a slightly different model. We neglect the environment of independent oscillators and its effect on the device. We are left with the oscillator, the in-built double dot and the SET. In this new frame we refer to the SET as the environment and the oscillator plus the double dot as the system. Following this, we reformulate the Hamiltonian as follows:

$$H = H_S + H_{\mathcal{E}} + H_I \tag{177}$$

where

$$H_S = \frac{\epsilon_{DD}}{2}\sigma_z + \frac{t}{2}\sigma_x + \hbar\omega_m a^\dagger a + g\sigma_z\hat{x} \tag{178}$$

$$H_{\mathcal{E}} = \epsilon_D\hat{n} + \sum_{k,\alpha}\xi_{\alpha k}c_k^\dagger c_k + \sum_{kk'}\left[t_{kk'}c_{kL}^\dagger c_{k'R} + \text{h.c.}\right] \tag{179}$$

$$H_I = g_c\hat{n}\sigma_z + g_x\hat{n}\hat{x} \tag{180}$$

Here we recall that the charge state of the dot expression $\hat{n} = d^\dagger d$. We aim now to estimate the sensitivity of the read out method to the displacement of the oscillator, to do so we focus on the case $\epsilon_{DD} = 0$ that is the most interesting, since we have seen previously that sensitivity is maximal for this case.

6.3. Expression for the current

In order to proceed we need to find the expression for the current. First we define the current:

$$I = \frac{d\langle N_L\rangle}{dt} \tag{181}$$

where we have the charge density operator $N_L = \sum_k c_{Lk}^\dagger c_{Lk}$. whose average is calculated in the interaction picture, resulting in:

$$I = \text{Tr}\left\{\dot{\rho}_I N_L(t) + \rho_I\dot{N}_L(t)\right\} \tag{182}$$

where $N_L(t) = U_0^\dagger(t)N_L U_0(t)$, $\rho = U_0(t)\rho_I U_0^\dagger(t)$, $H_0 = H_S + H_{\mathcal{E}}$. We now use the Von Neuman equation for the interaction picture density matrix ρ_I: $\dot{\rho}_I = -i[H_I(t), \rho_I]$, where the interaction Hamiltonian evolves with H_0. We insert the first order expression for the interaction picture density matrix:

$$\rho_I = \rho_I(0) - i\int_0^t dt'[H_I(t'), \rho(t')]. \tag{183}$$

Lastly the current operator can be defined as follows:

$$\hat{I} = \dot{N}_L = \frac{i}{\hbar}[H_0, N_L] = \frac{i}{\hbar}\sum_k t_\alpha\left[d^\dagger c_{Lk} - c_{Lk}^\dagger d\right] \tag{184}$$

discarding the dependence of t_L on k. The final expression of the current obtained at lowest order is:

$$I = -ig\int_0^t dt' \mathrm{Tr}_S\left\{x(t')\rho_S(t')\right\}\mathrm{Tr}_{\mathcal{E}}\left\{\rho_{\mathcal{E}}[\hat{I}(t), n(t')]\right\} = -ig\langle x\rangle\int_0^t dt'\langle[\hat{I}(t), n(t')]\rangle. \tag{185}$$

In physical terms, this consist in studying the linear response of the operator $\hat{I}$ to the external perturbation gxn. What is left is to calculate the average of the commutator, that can be explicited:

$$\langle[\hat{I}(t), n(0)]\rangle = it_L\sum_k \langle d^\dagger(t)c_k(t)d^\dagger d - c_k^\dagger(t)d(t)d^\dagger d - d^\dagger dd^\dagger(t)c_k(t) + d^\dagger dc_k^\dagger(t)d(t)\rangle. \tag{186}$$

Via the algebraic calculations each of these products can be decoupled, leaving:

$$\langle[\hat{I}(t), n(0)]\rangle = it_L\sum_k \left[\langle d^\dagger(t)d^\dagger\rangle\langle c_k(t)d^\dagger\rangle - \langle c_k^\dagger(t)d\rangle\langle d(t)d^\dagger\rangle - \langle d^\dagger c_k(t)\rangle\langle dd^\dagger(t)\rangle + \langle d^\dagger d(t)\rangle\langle dc_k^\dagger(t)\rangle\right] \tag{187}$$

Following the fact that the hermitian conjugation of a product of operators is the product of the hermitian conjugate of the operators with opposite order, we note that the first two terms in the parenthesis, as well as the last two, are one the hermitian conjugate of the other. Therefore Eq. (187) can be rewritten as:

$$\langle[\hat{I}(t), n(0)]\rangle = it_L\sum_k \left[2\,\mathbb{R}\mathrm{e}\left\{\langle d^\dagger(t)d\rangle\langle c_k(t)d^\dagger\rangle\right\} - 2\,\mathbb{R}\mathrm{e}\left\{\langle c_k^\dagger(t)d\rangle\langle d(t)d^\dagger\rangle\right\}\right] \tag{188}$$

In the following section we are going to present the result obtained from the calculation of these terms, yielding to a coefficient that is going to describe the proportionality between the displacement and the current.

Calculation of the correlators of the fermionic destruction and creation operators for electrons in the dot

We calculate here the correlation functions needed to obtain an expression for the current. For this purpose we will find the time evolution of the creation and annhilation fermionic operators. The electronic Hamiltonian of the single dot coupled to the leads reads:

$$H_e = \epsilon_D d^\dagger d + \sum_{k,\alpha}\xi_{\alpha k}c_k^\dagger c_k + \sum_{k,\alpha}\left[t_\alpha c_{\alpha k}^\dagger d \ + \mathrm{h.c.}\right]. \tag{189}$$

The Heisenberg equations of motions for the operators give:

$$\dot{d}(t) = i[H_e, d(t)] = -i\epsilon_D d(t) - i\sum_{k,\alpha} t_\alpha^* c_{\alpha k}(t) \tag{190}$$

$$\dot{c}_{\alpha k}(t) = i[H_e, c_{\alpha k}(t)] = -i\xi_{\alpha k}c_{\alpha k}(t) - it_\alpha d(t). \tag{191}$$

Introducing the rotating frame operators: $\tilde{d}(t) = d(t)e^{i\epsilon_D t}$ and $\tilde{c}_{\alpha k}(t) = c_{\alpha k}(t)e^{i\epsilon_D t}$ we rewrite the previous equations as:

$$\dot{\tilde{d}}(t) = -i\sum_{k,\alpha} t_\alpha^*\tilde{c}_{\alpha k}(t) \tag{192}$$

$$\dot{\tilde{c}}_{\alpha k}(t) = -i\Delta_{\alpha k}\tilde{c}_{\alpha k}(t) - it_\alpha\tilde{d}(t), \tag{193}$$

where $\Delta_{\alpha k} = (\xi_{\alpha k} - \epsilon_D)$. One approach is to solve Eq. (193) obtaining:

$$\tilde{c}_{\alpha k}(t) = -it_\alpha\int_0^t e^{-i\Delta_{\alpha k}(t-t')}d(t')dt' + e^{-i\Delta_{\alpha k}t}\tilde{c}_{\alpha k}(0), \tag{194}$$

that leads to:

$$\dot{\tilde{d}}(t) = -\sum_{k,\alpha}|t_\alpha|^2\int_0^t e^{-i\Delta_{\alpha k}(t-t')}d(t')dt' + \sum_{k,\alpha} it_\alpha^* e^{-i\Delta_{\alpha k}t}\tilde{c}_{\alpha k}(0). \tag{195}$$

Defining the density of states of the metallic leads, $\rho_\alpha(\omega) = \sum_k \delta(\omega - \Delta_{\alpha k})$ the summation over k can be replaced by integration.

$$\sum_{k,\alpha}|t_\alpha|^2\int_0^t e^{-i\Delta_{\alpha k}(t-t')}d(t')dt' = \sum_\alpha |t_\alpha|^2\int_0^t d(t')dt'\int_{-\infty}^{\infty} e^{i\omega(t'-t)}\rho_\alpha(\omega)d\omega \tag{196}$$

In the the wide-band approximation we assume the density of states constant, therefore the previous expression becomes:

$$\sum_\alpha 2\pi\rho_\alpha|t_\alpha|^2\int_0^t\delta(t'-t)d(t')dt' = \sum_\alpha 2\Gamma_\alpha\int_0^t\delta(t'-t)d(t')dt' = d(t)\sum_\alpha\Gamma_\alpha, \tag{197}$$

were we introduced the leads tunneling rates as $\Gamma_\alpha = \pi|t_\alpha|^2\rho_\alpha$. Also the second term of the left-hand side of the equation Eq. (195) can be rewritten, defining the incoming field as:

$$\tilde{c}_{\alpha,in}(t) = \sum_k e^{-i\Delta_{\alpha k}t}\tilde{c}_{\alpha k}(0). \tag{198}$$

Putting all together:

$$\dot{\tilde{d}}(t) = -\Gamma\tilde{d}(t) - \sum_\alpha ie^{i\phi_\alpha}\left(\frac{\Gamma_\alpha}{\pi\rho_\alpha}\right)^{1/2}\tilde{c}_{\alpha,in}(t) \tag{199}$$

where we defined $t_\alpha = |t_\alpha|e^{-i\phi_\alpha}$ and $\Gamma = \sum_\alpha 2\Gamma_\alpha$. We carry on by solving the equation in Fourier domain:

$$\tilde{d}(\omega) = -i\chi(\omega)\sum_\alpha e^{i\phi_\alpha}\left(\frac{\Gamma_\alpha}{\pi\rho_\alpha}\right)^{1/2}\tilde{c}_{\alpha,in}(\omega) \tag{200}$$

where $\chi(\omega) = (-i\omega+\Gamma)^{-1}$. This expression is interpretable as the response function to the external stimulus given by the incoming field, represented by the time evolution of the annihilation operator for the fermionic charge state in the metal. We can now compute the correlation functions beginning with:

$$\langle d^\dagger(t)d\rangle_\omega = |\chi(\omega)|^2\sum_\alpha\frac{\Gamma_\alpha}{\pi\rho_\alpha}\langle\tilde{c}^\dagger_{\alpha,in}(t)\tilde{c}_{\alpha,in}(0)\rangle_\omega \tag{201}$$

in which

$$\langle\tilde{c}^\dagger_{\alpha,in}(t)\tilde{c}_{\alpha,in}(0)\rangle = \sum_k e^{i\Delta_{\alpha k}t}\langle c^\dagger_{\alpha,k}(0)c_{\alpha,kin}(0)\rangle = \sum_k e^{i\Delta_{\alpha k}t}f_F(\xi_{\alpha k}-\mu_\alpha), \tag{202}$$

where f_F is the Fermi-Dirac distribution function. Substituting again the sum with an integral, introducing the density of states in the expression, one obtains:

$$\langle d^\dagger(t)d\rangle_\omega = |\chi(\omega)|^2\sum_\alpha\frac{\Gamma_\alpha}{\pi}\mathcal{F}\left[\int_{-\infty}^\infty e^{i\omega' t}f_F(\omega'+\epsilon_D-\mu_\alpha)d\omega'\right] \tag{203}$$

Which because of the properties of Fourier transform can be written as:

$$\langle d^\dagger(t)d\rangle_\omega = |\chi(\omega)|^2\sum_\alpha\Gamma_\alpha f_F(\epsilon_D-\mu_\alpha-\omega), \tag{204}$$

Let us define:

$$f_F(\epsilon_D-\mu_\alpha-\omega) = f_\alpha(\omega). \tag{205}$$

Now we have, in time domain:

$$\langle d^\dagger(t)d\rangle = \frac{1}{2\pi}\int_{-\infty}^\infty\frac{\sum_\alpha\Gamma_\alpha f_\alpha(\omega)}{\omega^2+\frac{\Gamma}{4}^2}e^{-i\omega t}d\omega, \tag{206}$$

Similarly, the following correlators can be computed:

$$\langle d^\dagger d(t)\rangle = \frac{1}{2\pi}\int_{-\infty}^\infty\frac{\sum_\alpha\Gamma_\alpha f_\alpha(-\omega)}{\omega^2+\frac{\Gamma}{4}^2}e^{-i\omega t}d\omega \tag{207}$$

$$\langle d(t)d^\dagger\rangle = \frac{1}{2\pi}\int_{-\infty}^\infty\frac{\sum_\alpha\Gamma_\alpha\left(1-f_\alpha(-\omega)\right)}{\omega^2+\frac{\Gamma}{4}^2}e^{-i\omega t}d\omega \tag{208}$$

$$\langle dd^\dagger(t)\rangle = \frac{1}{2\pi}\int_{-\infty}^\infty\frac{\sum_\alpha\Gamma_\alpha\left(1-f_\alpha(\omega)\right)}{\omega^2+\frac{\Gamma}{4}^2}e^{-i\omega t}d\omega \tag{209}$$

We proceed in computing the correlation functions between the fermionic operators of the metal and the dot.

Calculation of the correlators of the fermionic destruction and creation operators for electrons in the dot and in the metal leads

In light of Eq. (188) to proceed we need to evaluate $\langle c_k(t)d^\dagger\rangle$ and $\langle c_k^\dagger(t)d\rangle$. To do such a thing we first define some expression that will be useful in the following. From the equation of motion:

$$\dot{c}_{\alpha k}(t) \quad = \quad -i\xi_{\alpha k}c_{\alpha k}(t) - it_\alpha d(t), \tag{210}$$

Laplace transforming and switching to the rotating frame, this expression can be obtained:

$$\tilde{c}_{\alpha k}(\omega) = i\frac{c_{\alpha k}(0) - it_\alpha \tilde{d}(\omega)}{\omega - \Delta_{\alpha k} + i\eta}. \tag{211}$$

Equivalently, for its Hermitian conjugate:

$$\tilde{c}^\dagger_{\alpha k}(\omega) = i\frac{c_{\alpha k}(0) + it_\alpha \tilde{d}^\dagger(\omega)}{\omega + \Delta_{\alpha k} + i\eta}. \tag{212}$$

At this point we explicit the expression for the incoming field, see Eq. (198), in the Laplace domain:

$$\tilde{c}_{in,\alpha}(\omega) \quad = \quad \sum_k i\frac{c_{\alpha k}(0)}{\omega - \Delta_{\alpha k} + i\eta}, \tag{213}$$

$$\tilde{c}^\dagger_{in,\alpha}(\omega) \quad = \quad \sum_k i\frac{c^\dagger_{\alpha k}(0)}{\omega + \Delta_{\alpha k} + i\eta}, \tag{214}$$

that will later turn out to be useful. Knowing the time dependent expression of $\langle \tilde{c}^\dagger_{\alpha,in}(t)\tilde{c}_{\alpha,in}(0)\rangle$ from Eq. (202), and knowing that:

$$\langle c^\dagger_{\alpha,in}(\omega)c_{\alpha,in}(-\omega)\rangle = \int_{-\infty}^{\infty} dt e^{i\omega t}\langle c^\dagger_{\alpha,in}(t)c_{\alpha,in}(0)\rangle, \tag{215}$$

we have:

$$\langle c^\dagger_{\alpha,in}(\omega)c_{\alpha,in}(-\omega)\rangle = 2\pi\rho_\alpha f_\alpha(\omega). \tag{216}$$

We remind that we defined $f_F(-\omega + \epsilon_D - \mu_\alpha) \equiv f_\alpha(\omega)$. Analogously:

$$\langle c^\dagger_{\alpha,in}(-\omega)c_{\alpha,in}(\omega)\rangle \quad = \quad 2\pi\rho_\alpha f_\alpha(-\omega) \tag{217}$$

$$\langle c_{\alpha,in}(\omega)c^\dagger_{\alpha,in}(-\omega)\rangle \quad = \quad 2\pi\rho_\alpha(1 - f_\alpha(-\omega)) \tag{218}$$

$$\langle c_{\alpha,in}(-\omega)c^\dagger_{\alpha,in}(\omega)\rangle \quad = \quad 2\pi\rho_\alpha(1 - f_\alpha(\omega)) \tag{219}$$

We now have all the elements to compute the current. We want to first evaluate $it_L\sum_k\langle c^\dagger_{L,k}(t)d\rangle$, that given Eq. (212) and Eq. (200) can be rewritten in frequency domain as:

$$t_L\sum_k\langle c^\dagger_{L,k}(\omega)d(-\omega)\rangle = t_L\langle\left[\sum_k i\frac{c^\dagger_{L,k}(0) + it_L\tilde{d}^\dagger(\omega)}{\omega + \Delta_{L,k} + i\eta}\right]\tilde{d}(-\omega)\rangle. \tag{220}$$

In the first factor we recognize the expression for the incoming field, obtaining:

$$t_L\sum_k\langle c^\dagger_{L,k}(\omega)d(-\omega)\rangle = t_L\langle\left[c^\dagger_{L,in}(\omega) - \sum_k\frac{t_L\tilde{d}^\dagger(\omega)}{\omega + \Delta_{L,k} + i\eta}\right]\tilde{d}(-\omega)\rangle. \tag{221}$$

Taking advantage of the results from previously computed and bringing all together:

$$t_L\sum_k\langle c^\dagger_{L,k}(\omega)d(-\omega)\rangle = \frac{-\omega + i\frac{\Gamma}{2}}{\omega^2 + \frac{\Gamma}{4}^2}\Gamma_L f_L(\omega) - \sum_k\frac{t_L^2}{\omega + \Delta_{L,k} + i\eta}\frac{\sum_\alpha\Gamma_\alpha f_\alpha(\omega)}{\omega^2 + \frac{\Gamma}{4}^2}. \tag{222}$$

We proceed by separating the imaginary and real parts. We notice that in Eq. (188) the terms $\langle d^\dagger(t)d\rangle$ and $\langle d(t)d^\dagger\rangle$ are real, therefore we can discard the imaginary part in Eq. (222). Exploting Sokhotski–Plemelj theorem: $\sum_k\frac{t_L^2}{\omega\pm\Delta_{L,k}+i\eta} = \sum_k t_L^2 P\left(\frac{1}{\omega\pm\Delta_{K,L}}\right) - \frac{i\Gamma_L}{2}$ we obtain:

$$\mathbb{R}\mathrm{e}\{t_L\sum_k\langle c^\dagger_{L,k}(\omega)d(-\omega)\rangle\} = \frac{1}{\omega^2 + \frac{\Gamma}{4}^2}\left[-\omega\Gamma_L f_L(\omega) - \sum_k t_L^2 P\left(\frac{1}{\omega + \Delta_{K,L}}\right)\sum_\alpha\Gamma_\alpha f_\alpha(\omega)\right] \tag{223}$$

$\mathbb{R}\mathrm{e}\{t_L\sum_k\langle c_{L,k}(\omega)d^\dagger(-\omega)\rangle\}$ can be computed analogously. These expressions can be substituted inside Eq. (188), taking in to account Eq. (206) and Eq. (215), via a convolution integral eventually obtaining:

$$I = 2g\langle x\rangle\int\frac{d\omega}{2\pi}\frac{\omega\Gamma_L}{(\omega^2 + \frac{\Gamma}{4}^2)^2}\{\sum_\alpha\Gamma_\alpha f_\alpha(\omega)(1 - f_L(\omega)) + \sum_\alpha\Gamma_\alpha(1 - f_\alpha(\omega))f_L(\omega)\} \tag{224}$$

6.4. Semiclassical Calculation of the Current

Computing the current expression using a semiclassical treatment means calculating $\langle \hat{I} \rangle$, where $\hat{I}$ is the current operator previously defined. With similar calculation to what has been previously done, we have:

$$\langle I \rangle = \int \frac{d\omega}{2\pi} \frac{\Gamma_L \Gamma_R}{\omega^2 + \frac{\Gamma}{4}^2} (f_R(\omega) - f_L(\omega)), \tag{225}$$

If we now consider an energy level for the dot given by $\epsilon'_D(x) = \epsilon_D - xg$ in the spirit of a semi-classical treatment of the motion of the oscillator, assumed the shift to be small enough we expand the Fermi functions so to obtain:

$$\langle I \rangle = \int \frac{d\omega}{2\pi} \frac{\Gamma_L \Gamma_R}{\omega^2 + \frac{\Gamma}{4}^2} \left(f_R(\omega) - f_L(\omega) + \frac{xg}{k_B T} [f_L(\omega)(f_L(\omega) - 1) - f_R(\omega)(f_R(\omega) - 1)] \right). \tag{226}$$

We aim to compare this result with Eq. (224), which can be rewritten as

$$I = 2g\langle x \rangle \int \frac{d\omega}{2\pi} \frac{\omega \Gamma_L \Gamma_R}{(\omega^2 + \frac{\Gamma}{4}^2)^2} (f_L(\omega) - f_R(\omega)), \tag{227}$$

and integrated per parts:

$$I = \frac{g\langle x \rangle}{k_B T} \int \frac{d\omega}{2\pi} \frac{\Gamma_L \Gamma_R}{\omega^2 + \frac{\Gamma}{4}^2} (f_L(\omega)(f_L(\omega) - 1) - f_R(\omega)(f_R(\omega) - 1)), \tag{228}$$

which is precisely the correction term obtained by the semi-classical treatment, proving the validity of our calculations and assumptions since the results coincides.

6.5. Device sensitivity to displacement

At this point we may ask ourselves what is the sensitivity of the device under consideration, the single electron transistor, with respect to the oscillations of the carbon nanotube, i.e. how the current we just calculated is affected by the displacement. To evaluate such a figure of merit one could either consider the derivative of the expression of the current w.r.t. the position or the derivative of the conductance. We decided to go for the second option. To do such a thing we first have to retrieve a valid expression for the conductance. We begin again from the semi-classical expression of current

$$\langle I \rangle = \int \frac{d\omega}{2\pi} \frac{\Gamma_L \Gamma_R}{\omega^2 + \frac{\Gamma}{4}^2} (f_R(\omega) - f_L(\omega)), \tag{229}$$

where $f_{R,L}(\omega) = f_F(\epsilon_D - \mu_{L,R} - \omega)$. We now take into consideration the chemical potential of each of the two leads connected to the dot via tunneling junctions: $\mu_{L,R} = \mu_0 + \delta V_{L,R}$. For small potential bias of the two leads we can use the expansion of the Fermi distributions:

$$f_\alpha(\omega) = f_F(\omega) + f'_F(\omega) \delta V_\alpha \tag{230}$$

with $\alpha = R, L$ and $f_F(\omega) = f(\epsilon_D - \mu_0 - \omega)$. Substituting in the current expression the following is obtained:

$$I = \int \frac{d\omega}{2\pi} \frac{\Gamma_L \Gamma_R}{\omega^2 + \frac{\Gamma}{4}^2} f'_F(\omega)(\delta V_L - \delta V_R). \tag{231}$$

This is evidently the Ohm law for the SET quantum dot, in which the conductance is expressed by:

$$G = \int \frac{d\omega}{2\pi} \frac{\Gamma_L \Gamma_R}{\omega^2 + \frac{\Gamma}{4}^2} f'_F(\omega). \tag{232}$$

To evaluate the dependence of the conductance on the displacement, we have the dot energy given by $\epsilon'_D(x) = \epsilon_D - xg$, we consider small displacements to use the Fermi function derivative series expansion:

$$f'(\epsilon_D - xF_0 - \mu_0 - \omega) = f'(\epsilon_D - \mu_0 - \omega) - xg f''(\epsilon_D - \mu_0 - \omega). \tag{233}$$

Substituting this in the conductance expression leads to:

$$G = G_0 - xg \int \frac{d\omega}{2\pi} \frac{\Gamma_L \Gamma_R}{\omega^2 + \frac{\Gamma}{4}^2} f''(\epsilon_D - \mu_0 - \omega) \tag{234}$$

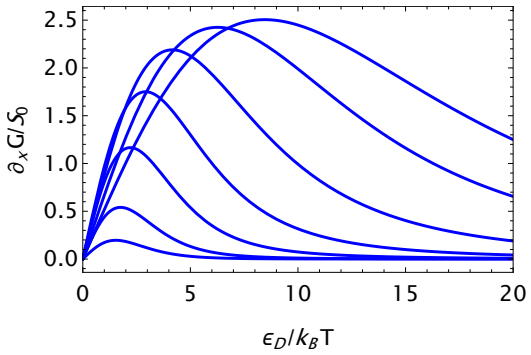

Figure 13: Device Sensitivity as a function of the dot energy from Eq. (236), for values of $\Gamma_1 = 1, 2, 4, 7, 12, 20, 28$

where $G_0 = \int \frac{d\omega}{2\pi} \frac{\Gamma_L \Gamma_R}{\omega^2 + \frac{\Gamma}{4}^2} f'_F(\omega)$. To have a measure of sensitivity we proceed by analyzing both analytically and numerically the derivative of conductance w.r.t displacement, i.e.

$$\frac{\partial G}{\partial x} = -F_0 \int \frac{d\omega}{2\pi} \frac{\Gamma_L \Gamma_R}{\omega^2 + \frac{\Gamma}{4}^2} f''(\epsilon_D - \mu_0 - \omega) \tag{235}$$

If we apply the following changes in variables: $y = \frac{\omega}{\Gamma/2}, \epsilon_1 = \frac{\epsilon_D - \mu_0}{k_B T}, \Gamma_1 = \frac{\Gamma}{k_B T}$ we get:

$$\frac{\partial G}{\partial x} = -\frac{F_0 \Gamma_L \Gamma_R}{\pi \Gamma^3} \Gamma_1^2 \int dy \frac{1}{y^2 + 1} f''(\epsilon_1 - \frac{\Gamma_1}{2} y). \tag{236}$$

In this way we wrote an expression composed by a constant which has the dimensions of a conductance over the displacement times an adimensional function:

$$S(\epsilon_1, \Gamma_1) = \Gamma_1^2 \int dy \frac{1}{y^2 + 1} f''(\epsilon_1 - \frac{\Gamma_1}{2} y). \tag{237}$$

The interesting part of this expression is the integral which has no trivial solution, so we decided to evaluate it numerically. The result will be compared to the analytical results obtained for two extreme cases, the one with $\Gamma_1 << 1$, physically meaning a state in which the thermal energy is high compared to the total tunneling rate related energy, and with $\Gamma_1 >> 1$, i.e. the opposite case. We note that usually in experiments the first condition is the one that occurs. Via numerical calculation we obtained the results displayed in Fig. 14 and Fig. 15, where the sensitivity is normalized on the constant value $S_0 = -F_0 \Gamma_L \Gamma_R / \pi \Gamma^3$. Also, we here show just half of the function since it is anti symmetric. As it is shown the max of the function increase with higher values of Γ_1, as expected, meaning that the lower is the temperature with respect to the tunneling rate energy the higher will be the accuracy in detecting the fluctuations of the current. Nonetheless we note that for values of Γ_1 higher than 10 the increase in sensitivity steadily slows down. To better understand this behaviour we approach the problem analytically distinguishing between two cases.
For high temperatures the above expression will be reduced to:

$$\left.\frac{\partial G}{\partial x}\right|_{\Gamma_1 \ll 1} = S_0 \pi \Gamma_1^2 f''(\epsilon_1), \tag{238}$$

given that in this conditions the Fermi distribution functions appearing in the integral could be considered smooth with respect to the Lorentzian. The maximum of this function is obtained for $\epsilon_1 = \log(2 - \sqrt{3})$, therefore:

$$\left.\frac{\partial G}{\partial x}\right|_{Max} = F_0 \frac{\Gamma_L \Gamma_R}{\Gamma^3} \frac{\Gamma_1^2}{6\sqrt{3}} = \frac{\Gamma_L \Gamma_R}{\Gamma (k_B T)^2} \frac{F_0}{6\sqrt{3}}, \tag{239}$$

For very high temperature the absolute value of the max sensitivity follows a quadratic relation w.r.t. Γ_1. It is worth to observe more deeply the behaviour of the maximum in this limiting case since this are the conditions realized experimentally (Fig. 13).
For very low temperatures, on the other hand, the fermi distribution functions could be considered peaked and integrating per parts we obtained:

$$\left.\frac{\partial G}{\partial x}\right|_{\Gamma_1 \gg 1} = S_0 \frac{8(\epsilon_1/\frac{\Gamma_1}{2})}{(1 + (\epsilon_1/\frac{\Gamma_1}{2})^2)^2} \tag{240}$$

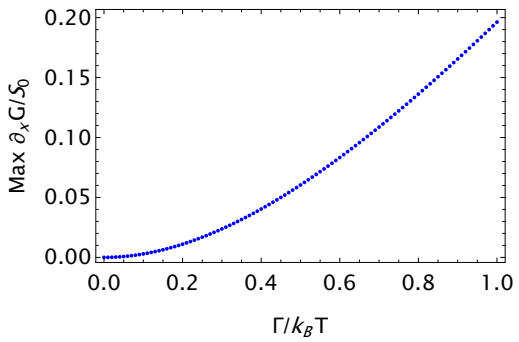

Figure 14: Max sensitivity of the device for values of Γ_1 from 0 to 1 with a 0.01 step

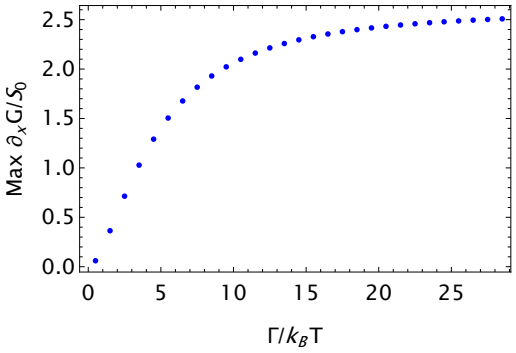

Figure 15: Max sensitivity of the device for values of Γ_1 from .5 to 28.5 with a 1 step

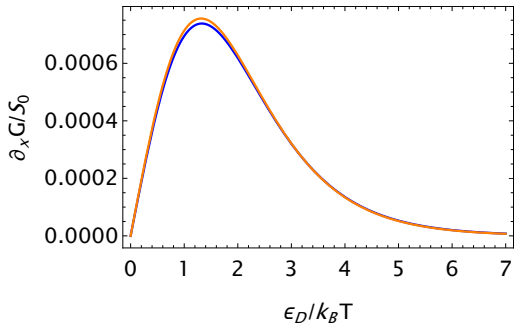

Figure 16: Comparison of the results obtained with the two methods of calculation, for a value of $\Gamma_1 = 0.05$

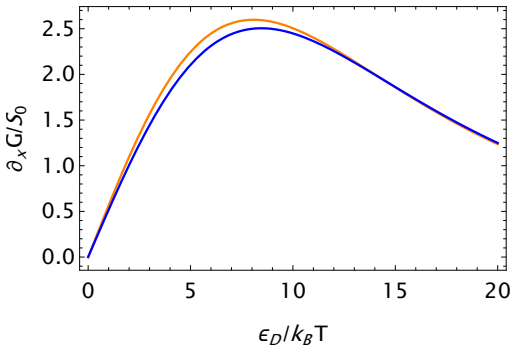

Figure 17: Comparison of the results obtained with the two methods of calculation, for a value of $\Gamma_1 = 28$

The First thing to be noted is that this expression does not depend on the temperature. Also this expression has its global maximum for $\epsilon_1 = \Gamma_1/2\sqrt{3}$, leading to:

$$\left.\frac{\partial G}{\partial x}\right|_{Max} = \frac{3\sqrt{3}}{2} S_0 = \frac{3\sqrt{3}}{2\pi} F_0 \frac{\Gamma_L \Gamma_R}{\Gamma^3} \tag{241}$$

The value of the maximum sensitivity is constant with respect to Γ_1, in agreement with the behaviour of the sensitivity function for high values of Γ_1 observed in numlerical results. The maximum sensitivity achievable therefore depends on phyisical values characteristic of the system i.e. the coupling F_0 and the tunneling rates. In particulare as expected the max sensitivity is proportional to the coupling constant in both the limiting conditions. Fig. 16 and Fig. 17 shows the agreement between the two methods of caclulation, with the numerical results (blue line) approaching the limiting case case for very low and very high Γ_1.

7. Conclusions

In conclusion, we investigated several aspects of the coupling between a set and a NMQbit. This was done mainly trough the analysis of the results in terms of parameters such as the coupling strength, tunneling rates, bias voltage and temperature.
At first we imposed the condition of the oscillator motion being much slower with respect to the tunneling rates which govern the current flow in the SET, given the typical experimental condition. This allowed a semiclassical treatment of the coupling, with the displacement of the oscillator being described exactly. Making use of the quantum linear response theory we were able to study the backaction of the SET metallic island charge state on the oscillator, retrieving the expression of the induced effective temperature. The main result were the exponential dependence of the effective temperature on the bias voltage applied to the SET, and the independence of the maximum fluctuation value on the voltage. Furthermore we demonstrated the impact of the energy level of the metallic island since by adjusting it with a gate voltage it is possible to control the tunneling rates too.

We then went on with the calculation of the current expression, in order to study the sensitivity of the device. To do so we proceeded with both a full quantum description at first order and a semiclassical treatment, obtaining the same result. From the expression of the current we computed the conductance, and given its derivative with respect to the position we obtained a measure of the sensitivity. The behaviour of this figure of merit was explored by adjusting different parameters, of which we highlighted the bias voltage, the temperature and the tunneling rates. The maximum gain in sensitivity was showed for high tunneling rates with respect to the temperature, up to a certain threshold $\hbar\Gamma \simeq 10k_BT$ after which the gain in sensitivity is dumped presumably by the strong backaction that would act on the oscillator for high currents in the SET. As a last remark, the sensitivity showed to be directly proportional to the coupling between the metallic island charge state and the oscillator.
Our work contributes to the understanding of the operations of this device composed of a SET and a NMQbit, that could have the potential for quantum computing applications. With these results one could aim to tune its device in an operation regime suitable to perform a read out of the NMQubit preserving its coherence, given its quality factor and decoherence rates. Further research can explore the optimization of the system parameters and the integration with other quantum technologies to realize practical quantum computing devices. Another possible development is the study of the second order quantum treatment which may lead to a different expression for current with respect to the semiclassical one. On a more technical note, a possible future development could be to compute the noise generating from the current, i.e. the noise associated to conductance, in a similar fashion to what was done with the charge state in section 5.2.

References

[1] Yoonjin Won, Yuan Gao, Matthew A Panzer, Senyo Dogbe, Lawrence Pan, Thomas W Kenny, and Kenneth E Goodson. Mechanical characterization of aligned multi-walled carbon nanotube films using microfabricated resonators. *Carbon*, 50(2):347–355, 2012.

[2] Vladimir Borisovich Berestetskii, Evgenii Mikhailovich Lifshitz, and Lev Petrovich Pitaevskii. *Quantum Electrodynamics: Volume 4*, volume 4. Butterworth-Heinemann, 1982.

[3] Richard P Feynman. Simulating physics with computers. In *Feynman and computation*, pages 133–153. CRC Press, 2018.

[4] David Deutsch. Quantum theory, the church–turing principle and the universal quantum computer. *Proceedings of the Royal Society of London. A. Mathematical and Physical Sciences*, 400(1818):97–117, 1985.

[5] Peter W Shor. Algorithms for quantum computation: discrete logarithms and factoring. In *Proceedings 35th annual symposium on foundations of computer science*, pages 124–134. Ieee, 1994.

[6] Charles H Bennett and Gilles Brassard. Quantum cryptography: Public key distribution and coin tossing. *arXiv preprint arXiv:2003.06557*, 2020.

[7] William K Wootters and Wojciech H Zurek. A single quantum cannot be cloned. *Nature*, 299:802–803, 1982.

[8] Giuliano Benenti, Giulio Casati, and Giuliano Strini. *Principles of quantum computation and information-volume I: Basic concepts*. World scientific, 2004.

[9] Giuliano Benenti, Giulio Casati, and Giuliano Strini. *Principles of quantum computation and information-volume I: Basic concepts*. World scientific, 2004.

[10] Maximilian A Schlosshauer. *Decoherence: and the quantum-to-classical transition*. Springer Science & Business Media, 2007.

[11] Giuliano Benenti, Giulio Casati, and Giuliano Strini. *Principles of Quantum Computation and Information-Volume II: Basic Tools and Special Topics*. World Scientific Publishing Company, 2007.

[12] Tsuyoshi Yamamoto, Yu A Pashkin, Oleg Astafiev, Yasunobu Nakamura, and Jaw-Shen Tsai. Demonstration of conditional gate operation using superconducting charge qubits. *Nature*, 425(6961):941–944, 2003.

[13] Franco Ciccacci et al. *Fondamenti di fisica atomica e quantistica*. EdiSES, 2012.

[14] Stephan GJ Philips, Mateusz T Mądzik, Sergey V Amitonov, Sander L de Snoo, Maximilian Russ, Nima Kalhor, Christian Volk, William IL Lawrie, Delphine Brousse, Larysa Tryputen, et al. Universal control of a six-qubit quantum processor in silicon. *Nature*, 609(7929):919–924, 2022.

[15] Christian L Degen, Friedemann Reinhard, and Paola Cappellaro. Quantum sensing. *Reviews of modern physics*, 89(3):035002, 2017.

[16] Gregory S MacCabe, Hengjiang Ren, Jie Luo, Justin D Cohen, Hengyun Zhou, Alp Sipahigil, Mohammad Mirhosseini, and Oskar Painter. Nano-acoustic resonator with ultralong phonon lifetime. *Science*, 370(6518):840–843, 2020.

[17] Carlos Urgell, Wei Yang, Sergio Lucio De Bonis, Chandan Samanta, Maria José Esplandiu, Quan Dong, Yong Jin, and Adrian Bachtold. Cooling and self-oscillation in a nanotube electromechanical resonator. *Nature Physics*, 16(1):32–37, 2020.

[18] Frank Arute, Kunal Arya, Ryan Babbush, Dave Bacon, Joseph C Bardin, Rami Barends, Rupak Biswas, Sergio Boixo, Fernando GSL Brandao, David A Buell, et al. Quantum supremacy using a programmable superconducting processor. *Nature*, 574(7779):505–510, 2019.

[19] S Rips, I Wilson-Rae, and MJ Hartmann. Nonlinear nanomechanical resonators for quantum optoelectromechanics. *Physical Review A*, 89(1):013854, 2014.

[20] F Pistolesi, AN Cleland, and A Bachtold. Proposal for a nanomechanical qubit. *Physical Review X*, 11(3):031027, 2021.

[21] Pasquale Scarlino, David J Van Woerkom, Anna Stockklauser, Jonne V Koski, Michele C Collodo, Simone Gasparinetti, Christian Reichl, Werner Wegscheider, Thomas Ihn, Klaus Ensslin, et al. All-microwave control and dispersive readout of gate-defined quantum dot qubits in circuit quantum electrodynamics. *Physical review letters*, 122(20):206802, 2019.

[22] Fabio Pistolesi. Bistability of a slow mechanical oscillator coupled to a laser-driven two-level system. *Physical Review A*, 97(6):063833, 2018.

[23] Aashish A Clerk and Steven Bennett. Quantum nanoelectromechanics with electrons, quasi-particles and cooper pairs: effective bath descriptions and strong feedback effects. *New Journal of Physics*, 7(1):238, 2005.

[24] Aashish A Clerk, Michel H Devoret, Steven M Girvin, Florian Marquardt, and Robert J Schoelkopf. Introduction to quantum noise, measurement, and amplification. *Reviews of Modern Physics*, 82(2):1155, 2010.

[25] Christian Barthel, Morten Kjærgaard, J Medford, Michael Stopa, Charles Masamed Marcus, MP Hanson, and Arthur C Gossard. Fast sensing of double-dot charge arrangement and spin state with a radio-frequency sensor quantum dot. *Physical Review B*, 81(16):161308, 2010.

A. Appendix: Derivation of the bias and gate voltage dependence of rates

We begin by writing the Fermi golden rule tunnel rate expression from a metal to a single level dot:

$$\Gamma^{+}_{L,R} = \frac{2\pi}{\hbar}\sum_i |M_{if}|^2 P_i \delta(E_i - E_f) \tag{242}$$

where M_{if} is the tunnelling matrix element, that we will take as constant, P_i the probability of the initial state, and E_i and E_f are the initial and final energy of the full electronic system, including the Coulomb electrostatic energy. We can thus write

$$E_i = \epsilon_k + E^C_i \qquad E_f = \epsilon_D + E^C_f \tag{243}$$

where ϵ_k and ϵ_D are the quantum level energy and E^C the total Coulomb energy. Given the scheme of which in section 4.3, the difference between coulomb energies reads:

$$\Delta E^C_{L,R} = E^C_f - E^C_i = \frac{(Q-e)^2}{2C_\Sigma} - \frac{Q^2}{2C_\Sigma} - e\sum_l \frac{C_l}{C_\Sigma}(V_l - V_{L,R}) \tag{244}$$

this expression corresponds to adding one electron from left or right lead on the central island, V_l for $l = L, R, g$ are the potential of the three leads, left, right and gate. We can now write explicitly the difference of energy:

$$\Delta E_L^+ = E_f - E_i = \epsilon_D - \epsilon_k + \frac{e^2 - 2Qe}{2C_\Sigma} - ec_g(V_g - V_L) - ec_R(V_R - V_L) \quad (245)$$

$$, \Delta E_R^+ = E_f - E_i = \epsilon_D - \epsilon_k + \frac{e^2 - 2Qe}{2C_\Sigma} - ec_g(V_g - V_R) - ec_L(V_L - V_R). \quad (246)$$

where we defined $c_l = C_l/C_\Sigma$. The probability entering the Fermi golden rule is simply the Fermi function:

$$P_i = f_F(\epsilon_k) = \frac{1}{e^{\epsilon_k/T} + 1} \quad (247)$$

we can now integrate the energy ϵ_k explicitly and obtain

$$\Gamma_L^+ = \frac{2\pi}{\hbar}\rho|M|^2 f_F[\epsilon_1 - ec_g(V_g - V_L) - ec_R(V_R - V_L)] \quad (248)$$

$$\Gamma_R^+ = \frac{2\pi}{\hbar}\rho|M|^2 f_F[\epsilon_1 - ec_g(V_g - V_R) - ec_L(V_L - V_R)] \quad (249)$$

where $\epsilon_1 = \epsilon_D + \frac{e^2-2Qe}{2C_\Sigma}$. Being this term constant can be neglected in the following, by acting on the zero of the gate voltage. In the experiment one of the two leads is set to 0 and the other to V, and the gate voltage is measured with respect to the 0. Choosing $V_R = 0$, defining $v = eV_L/T$ and $v_g = eV_g/T$ we have

$$\Gamma_L^+ = \Gamma_L^0 f(-c_g v_g + (c_R + c_g)v) = \Gamma_L^0 f_L, \quad (250)$$

$$\Gamma_R^+ = \Gamma_R^0 f(-c_g v_g - c_L v) = \Gamma_R^0 f_R \quad (251)$$

with $f(x) = 1/(e^x + 1)$. From these expressions the expressions for Γ^- can be rapidly derived using the fact that they are the reversed process, thus the variation of the energy is minus the one we found.:

$$\Gamma_L^- = \Gamma_L^0[1 - f(-c_g v_g + (c_R + c_g)v)] = \Gamma_L^0(1 - f_L), \quad (252)$$

$$\Gamma_R^- = \Gamma_R^0[1 - f(-c_g v_g - c_L v)] = \Gamma_R^0(1 - f_R). \quad (253)$$

Abstract in lingua italiana

I recenti sviluppi degli oscillatori nanomeccanici li pongono come interessante alternativa per l'implementazione dei computer quantistici. Recentemente, è stata proposta la realizzazione di un qubit nanomeccanico nella forma di un nanotubo di carbonio, i cui modi di oscillazione sono accoppiati a un doppio quantum dot integrato nel nanotubo stesso. In questo lavoro, puntiamo a studiare uno dei possibili metodi di lettura dello stato di questo oscillatore meccanico, attraverso un transistor a singolo elettrone (SET). Quest'ultimo si compone di una isola metallica micrometrica isolata dal resto del circuito attraverso due tunneling junctions. Questo schema permette il passaggio di un elettrone per volta, il che lo rende in principio adatto come dispositivo di lettura ad alta sensitività. Qui calcoliamo la retroazione del SET sull'oscillatore, presentando l'eccitazione di quest'ultimo per mezzo della temperatura efficace. Dimostriamo l'andamento esponenziale della temperatura efficace in funzione della tensione di bias applicata al SET. Inoltre ricaviamo la dipendenza della temperatura efficace dal livello energetico dell'isola metallica del SET. A seguire, calcoliamo l'espressione della corrente nel SET ottenendo la dipendenza dalla posizione dell'oscillatore. Questo calcolo viene fatto sia in approssimazione semiclassica sia con una descrizione pienamente quantistica. Formuliamo la sensitività del SET nei termini della derivata della conduttanza rispetto allo spostamento dell'oscillatore ed esprimiamo questa figura di merito come funzione del livello energetico dell'isola metallica e del rate di tunneling nel SET. Questo ci permette di stimare il comportamento del dispositivo per diversi regimi operativi, caratterizzati da parametri quali la tensione di bias applicata nel SET e altri valori fisici caratteristici del sistema oscillatore-SET.

Parole chiave: oscillatore nanomeccanico, nanotubo di carbonio, transistor a singolo elettrone, qubit

Acknowledgements

I acknowledge support from the Politecnico di Milano, CNRS, LOMA, professor Fabio Pistolesi and professor Andrea Crespi.